



FINAL PUBLISHABLE JRP REPORT

JRP-Contract number	EXL03	
JRP short name	MICROPHOTON	
JRP full title	Measurement and control of single-photon microwave radiation on chip	
Version numbers of latest contracted Annex Ia and Annex Ib against which the assessment will be made	Annex Ia:	V1.3
	Annex Ib:	V1.01
Period covered (dates)	From 1 June 2013	To 31 May 2016
JRP-Coordinator		
Name, title, organisation	Antti Manninen, Dr., Teknologian tutkimuskeskus VTT Oy	
Tel:	+358 40 514 8658	
Email:	antti.manninen@vtt.fi	
JRP website address	www.microphoton.eu	
Other JRP-Partners		
Short name, country	INRIM, Italy	
	NPL, United Kingdom	
	PTB, Germany	
REG-Researcher (associated Home Organisation)		
Researcher name, title (Home organisation Short name, country)	Mikko Möttönen, Professor Aalto, Finland	Start date: 1 June 2013 Duration: 36 months
Researcher name, title (Home organisation Short name, country)	Yuri A. Pashkin, Professor LanU, UK	Start date: 1 June 2013 Duration: 36 months
Researcher name, title (Home organisation Short name, country)	Phil Meeson, Dr. RHUL, UK	Start date: 1 Jan 2014 Duration: 24 months

Report Status: PU Public

EXL03 MICROPHOTON



Researcher name, title
(Home organisation Short
name, country)

Oleg Astafiev, Professor
RHUL, UK

Start date: 1 Nov 2013
Duration: 18 months

TABLE OF CONTENTS

1	Executive Summary	4
2	Project context, rationale and objectives.....	5
2.1	Project context and rationale	5
2.2	Objectives	5
3	Research results.....	6
3.1	Objective 1: Development of single-microwave photon detectors which give spectral information about radiation. Sensors will be developed to cover a wide frequency range from below 10 GHz up to about 300 GHz. The methods will be based on superconductor and semiconductor nanodevice technologies.	6
3.1.1	Detectors based on single-electron effects in superconductor-insulator-normal metal structures	6
3.1.2	Semiconductor quantum-dot detectors	8
3.1.3	SNS detectors	10
3.1.4	Bifurcation amplifier	12
3.1.5	Summary of microwave photon detectors	14
3.2	Objective 2: Development of cryogenic sources of microwave photons to cover frequencies between 4 GHz and 300 GHz – a single-photon source based on a superconducting qubit, and other microwave photon sources based on biased Josephson junctions and on black-body radiation – and their use in the characterisation of the developed photon detectors.....	14
3.2.1	Single-photon source based on a superconducting transmon qubit	14
3.2.2	Tuneable single-photon source based on a tuneable gap flux qubit.....	17
3.2.3	Josephson junction photon source.....	20
3.2.4	Thermal photon source	22
3.2.5	Josephson junction photon source coupled with SINIS and NISIN detectors	24
3.2.6	Superconducting transmon qubit -based source and SNS detector	27
3.2.7	Summary of microwave photon sources	28
3.3	Objective 3: Characterisation and minimisation of background microwave radiation in the cryogenic measurement systems of nanoelectronic devices. The goal is to decrease the background microwave radiation to a level which corresponds to the voltage noise of a SINIS-SET much below $1 \text{ pV/Hz}^{1/2}$ at frequencies above 10 GHz, simultaneously allowing bandwidth up to about 10 GHz for the control signals from room temperature to the cryo-electronic device. .	29
3.3.1	Summary of research on background microwave radiation in cryogenic environments	30
3.4	Objective 4: Demonstrations of the improved performance of cryoelectronic quantum nanodevices such as SINIS-SET-based components and other devices in which perfectness of superconductivity is important.	31
3.4.1	Summary of research on improved performance of SINIS-SET based components	32
3.5	Summary of research results.....	32
4	Actual and potential impact	34
5	Website address and contact details	35
6	List of publications	35

1 Executive Summary

Introduction

Applications of quantum technology are expanding in fields such as medical imaging (e.g. magnetoencephalography), airport security and telecommunications. Single-photon microwave sources and detectors are examples of precisely controllable quantum devices needed especially in quantum information processing and communication (QIPC). The lack of such sources and detectors has been a major limitation, for instance in QIPC based on circuit quantum electrodynamics (cQED). To address this need, this project developed several types of microwave detectors and sources suitable for operation at the single (or near single) photon level. Quantum devices are operated at cryogenic environments, as the quantum mechanical nature of materials becomes most apparent at low temperatures. Therefore the project provided tools for cryogenic experiments that will lead to a better understanding of quantum devices and thus improve their performance.

The Problem

In the ongoing second quantum revolution, new types of quantum devices are being developed that promise unprecedented capabilities for a wide range of applications. One especially active and important research field is the development of QIPC using quantum bits (qubits) based on superconducting devices. Microwave photon sources and detectors are important elements for superconductor-based QIPC. However, at the start of the project, 'on-demand' generation of single microwave photons had been demonstrated in only few experiments, and single-photon detectors for microwave frequencies were not available at all.

Residual microwave photons are a serious problem for many cryogenic quantum devices. An ultraquiet microwave environment minimising noise and thermally excited microwave photons as well as ultrasensitive measurement methods are needed to study and minimise the effects of background microwave radiation on quantum nanodevices in cryogenic environments.

The Solution

In this project, the consortium developed several types of cryogenic microwave detectors and sources suitable for operation at the single (or near single) photon level, as well as tools for characterising the effects of background microwave radiation on quantum nanodevices in cryogenic environments. Results include:

- realisation and proof-of-principle operation of a period-doubling bifurcation (PDB) amplifier;
- order-of-magnitude improvement of microwave photon detection sensitivity of thermal detectors;
- demonstration of the operation of a novel superconducting qubit device as an on-demand source of single microwave photons with a tuneable frequency;
- observation of enhanced photon-assisted single-electron tunnelling rates in a SINIS single-electron trap when the trap is radiated by an on-chip microwave source;
- use of a SINIS trap detector and cryogenic microwave background radiation as tools for characterising spectral properties of superconducting on-chip filters at microwave frequencies.

Impact

The impact of this project is mostly in the scientific community, however, in the long-term, there will be financial and social impacts. The cryoelectronics market has already a significant volume of commercial applications, and this is expected to increase dramatically in future as the recent progress in cryogen-free refrigeration and on-chip coolers is making cryoelectronics more attractive for practical applications. Easy-to-use commercial methods for signal line filtering and radiation shielding of quantum nanodevices will benefit the manufacturers of cryogenic refrigerators and components.

To maximise the scientific impact, many of the results have been published in highly ranked scientific journals such as Nature Communications and Physical Review Letters. Altogether, the project has resulted in 19 peer-reviewed publications and proceedings. A more general article about controlling single microwave photons was published in the Microwave Journal, which reaches 50,000 readers from all over the world. Project results have also been presented in 47 presentations or posters at scientific conferences and workshops. In addition, the MICROPHOTON 2016 workshop was arranged, the project website www.microphoton.eu was set up, and a good practice guide for microwave radiation detection, shielding and filtering within cryogenic systems was produced.

Even though single-photon real-time detection with good fidelity was not achieved during the lifetime of the project, the achievement of this end goal is now closer. The microwave photon detectors and sources developed in this project have the potential to enable the realisation of a practical quantum computer based on solid-state qubits, which would be a revolutionary breakthrough.

2 Project context, rationale and objectives

2.1 Project context and rationale

In the quantum revolution, new types of quantum devices are being developed that promise unprecedented capabilities for a wide range of applications. One particularly active and important research field is the development of quantum information processing and communication (QIPC) using quantum bits (qubits) based on superconducting devices and other cryoelectronic components.

The development of any future superconducting quantum computing technology will depend on the availability of on-chip single-photon and few-photon microwave components. Yet, electromagnetic metrology for microwave frequencies at very small signal levels is still in its infancy.

Quantum device technology requires the development of microwave photon detectors and sources at the single-photon level. Photons at microwave frequencies offer advantages over optical frequencies as normal microwave components can be used together with special superconducting electronics. For example, in QIPC single microwave photons can be generated and used as qubits in quantum computing and measured using single-photon detectors. Thus, 'on-demand' sources of microwave photons with known qualities, and detection of these photons in a reliable way at the single-photon level is essential.

At the start of this project, 'on-demand' generation of single microwave photons had been demonstrated in only a few experiments, and single-photon detectors for microwave frequencies were not available at all. This was because the energy of a microwave photons is much lower than that of optical photons, meaning that detection of microwave photons at the quantum level needs extremely sensitive detectors operating in ultra-low noise environments.

The development of such cryonanoelectronic devices requires ultrasensitive microwave sensors to tackle the problem of the residual microwave photons, which can distort measurements. An ultraquiet microwave environment minimising noise and thermally excited microwave photons is needed to study the effects of background microwave radiation on quantum nanodevices in cryogenic environments.

2.2 Objectives

The objectives of this project included the development of novel microwave detectors and sources down to the single-photon level, and the improvement in the performance of cryoelectronic quantum devices by understanding and eliminating the detrimental effects caused by microwave radiation coming from the electromagnetic environment. The specific objectives were:

- Development of single-microwave-photon detectors which give spectral information about radiation. Sensors will be developed to cover a wide frequency range from below 10 GHz up to about 300 GHz. The methods will be based on superconductor and semiconductor nanodevice technologies.
- Development of cryogenic sources of microwave photons to cover frequencies between 4 GHz and 300 GHz – a single-photon source based on a superconducting qubit, and other microwave photon sources based on biased Josephson junctions and on black-body radiation – and their use in the characterisation of the developed photon detectors.
- Characterisation and minimisation of background microwave radiation in the cryogenic measurement systems of nanoelectronic devices. The goal is to decrease the background microwave radiation to a level which corresponds to the voltage noise of a SINIS-SET much below $1 \text{ pV/Hz}^{1/2}$ at frequencies above 10 GHz, simultaneously allowing bandwidth up to about 10 GHz for the control signals from room temperature to the cryo-electronic device.
- Demonstrations of the improved performance of cryoelectronic quantum nanodevices such as SINIS-SET-based components and other devices in which perfectness of superconductivity is important.

3 Research results

3.1 Objective 1: Development of single-microwave photon detectors which give spectral information about radiation. Sensors will be developed to cover a wide frequency range from below 10 GHz up to about 300 GHz. The methods will be based on superconductor and semiconductor nanodevice technologies.

As explained in Section 2.2, the first objective of the project required different solutions to be developed for microwave photon detection for different frequency ranges from below 10 GHz up to 300 GHz. Detectors based on single-electron effects in superconductor - normal metal and semiconductor nanodevices were developed for frequencies above 50 GHz. SNS detectors were also developed for frequencies between about 10 GHz - 80 GHz, and bifurcation amplifiers for frequencies below about 20 GHz.

3.1.1 Detectors based on single-electron effects in superconductor-insulator-normal metal structures

An important milestone of the project was the detailed characterisation of properties of the SINIS-type (Superconductor - Insulator - Normal metal - Insulator - Superconductor) single-electron traps as detectors of single microwave photons [10]. In experiments at PTB, this type of detector, based on two ultra small Al/Ox/AuPd tunnel junctions, was found to be able to detect photons in the frequency range from below 100 GHz up to about 180-200 GHz for the counting rates $\Gamma \sim 1 \div 50 \text{ s}^{-1}$. This frequency range is important e.g. for the characterisation of the microwave background in cryogenic environments. Due to the large impedance mismatch between the SINIS transistor and the electromagnetic environment, the quantum efficiency of the SINIS-type photon detectors is very small, i.e., only a small fraction of incoming photons is actually absorbed. One of the benefits is that spectral information about the microwave radiation can be obtained by adjusting the threshold energy for single-electron tunnelling (SET).

The detection mechanism involves the so-called photon-assisted tunnelling (PAT) effect in SET circuits. PTB developed several variations of the detector, and most of them are based on the SINIS single-electron trap (see the equivalent circuit and an example of a fabricated device in Figure 3.1.1.1.). Its operating principle is based on detecting single absorbed photons by observing the photon-assisted tunnelling events of electrons. If the energy of the photon is higher than the SINIS trap's threshold energy it can be adjusted by external voltages. The absorption of the photon delivers enough energy to cause recharging or charging of the trap by a single electron. That charge change is registered by the SINIS electrometer as shown in Figure 3.1.1.1c. The time resolution of the detector circuit is limited by the RC-constant of the dc-SET transistor on the scale of milliseconds, thus limiting the secure range of counting rates below about 100 counts per second. PTB tested the SINIS trap extensively using on-chip Josephson junctions as the microwave source (see Section 3.2.5), and VTT used one version of the SINIS trap in measurements of the on-chip filtering of the background microwave radiation (see Section 3.3.1).

Figure 3.1.1.1d demonstrates the use of the SINIS trap as a detector of microwave background photons. At low temperatures, the rate of tunnelling events is dominated by the microwave background photons and the PAT effect, and the SINIS trap can be used as a microwave photon detector. In this region, the hold time (or tunnelling rate) of electrons in the trap depends strongly on the threshold energy of the trap, as only photons whose energy $E_{\text{ph}} = hf$ (h is Planck's constant, f is microwave photon frequency) is larger than the threshold energy can cause tunnelling events. In this way, the measurements give information about the spectrum of the microwave photon background.

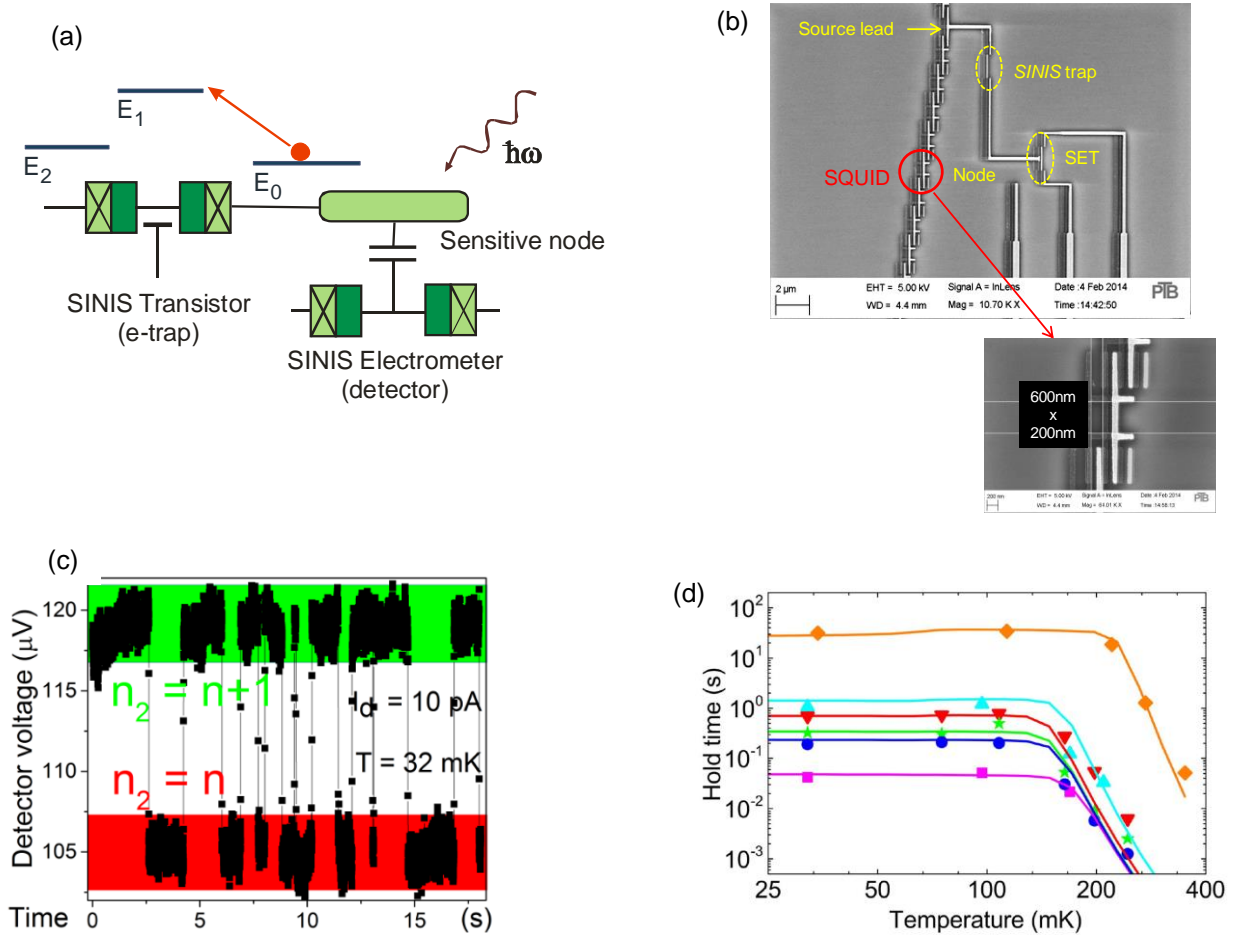


Figure 3.1.1.1. (a) The equivalent circuit of the SINIS trap detector. When a photon is absorbed, the charge state of the sensitive node can change by a single electron due to photon-assisted tunnelling in the two-junction SINIS transistor (e-trap) of the circuit. The charge state of the node is constantly monitored by the SINIS electrometer made using the same technique as the trap. (b) A scanning electron micrograph on a sub-100- μm scale showing a SINIS trap-detector with the charge node monitored by a SINIS SET electrometer. The microwaves from the electromagnetic background are coupled to the detector via a SQUID-array filter with up to 40 SQUIDs in a chain. The device was designed and fabricated by PTB. (c) An example of the SINIS SET electrometer signal showing transitions between two charge states (n electrons or $n+1$ electrons) in the sensitive node of the detector. Transitions between charge states are due to photon-assisted tunnelling caused by absorbed microwave photons. (d) VTT's measurements of the temperature dependence of the hold time of the trapped electrons at different values of the SINIS trap's threshold energy ΔE for electron tunnelling, varying between 69 GHz (magenta squares) and 165 GHz (orange diamonds) in terms of threshold frequency $f_{th} = \Delta E/h$, where h is Planck's constant [16].

With conventional methods, the time resolution of the SINIS trap detector circuit is limited by the RC-constant of the SINIS SET electrometer on the scale of milliseconds, thus limiting the secure range of counting rates below 100 photons per second. To detect more intensive microwave irradiation, with up to ~ 1000 photons absorbed per unit time (s), the group at PTB implemented a variation of the SINIS detector. It is based on a NISIN SET transistor in which the superconducting and normal metal parts of the SINIS detector are transposed. A simple device based on a two-junction arrangement of a NISIN SET transistor with a superconducting island was implemented [9]. In the Coulomb blockade state, the dc leak current through the device provided a sensitive measure of the microwave radiation absorbed. A remarkable feature of this circuit appears as a photo-electron multiplication effect. This appears to be due to an unpaired quasiparticle in the transistor island: the effect is illustrated in Figure 3.1.1.2.

PTB analysed the performance of the NISIN detector and, in particular, estimated the value of the multiplication gain as being ~ 1000 and the saturation number as being ~ 1000 photons absorbed per second, thus extending the range of photon absorption by an order of magnitude as compared to the SINIS trap detector [9]. The high gain value helps to achieve a low detection threshold of about 50 photons per second, mostly limited by the fA-current resolution of the measuring amplifier operating at room temperature.

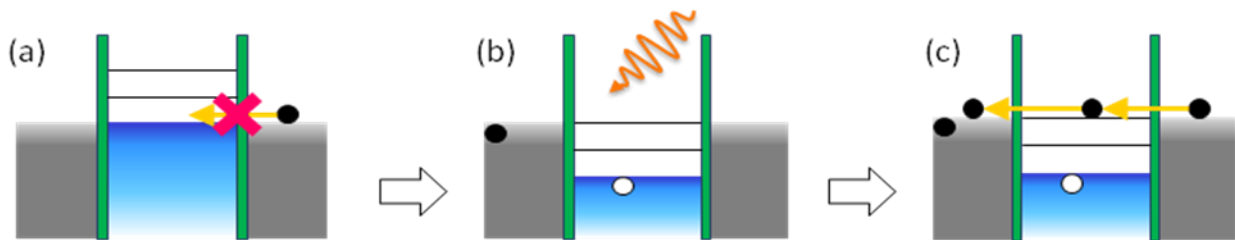


Figure 3.1.1.2. Operation principle of the NISIN SET detector illustrated using an energy diagram of two normal conducting leads (grey banks right and left) separated from the (blue-coloured) superconducting island in the middle by tunnel barriers (green bars). (a) No tunnelling is possible in the Coulomb blockade state. (b) Absorption of a microwave photon leads to excitation of an unpaired quasiparticle in the island, and (c) that provides a favourable condition for single-quasiparticle current through the island. The charge transfer sequence lasts until two quasiparticles recombine in the island at a time scale of about 1 ms.

A similar detection mechanism with comparable parameters was demonstrated for a fully-superconducting SISIS detector, based however on a more complex Cooper-pair-quasiparticle cotunnelling mechanism of the photon-induced current. Differently from the NISIN device, a higher energy activation threshold was observed, accounting for excitation of two quasiparticles (due to both junction electrodes being superconducting) by the incident photon and making the SISIS device more attractive to detect microwave radiation in the frequency range above 100 GHz.

3.1.2 Semiconductor quantum-dot detectors

The development of microwave photon detectors for frequencies above tens of gigahertz (GHz) is important as this frequency range, especially from about 100 GHz up to a few terahertz (THz), is exploited for applications such as medical imaging and security search. In this frequency range, semiconductor-based detectors are promising candidates, as the operation of superconductor-based detectors, although more widely used, are often limited to lower frequencies. Semiconductor-based detectors also have advantages, when microwave detections needed to be resolved at a single-photon level, as the state-of-the-art device fabrication and operation technologies enable single-electron device operation; a single-photon detection becomes possible by the detection of an energy excitation of one electron which absorbs one photon. Microwave photon detection has been achieved using semiconductor quantum dots containing a large number of electrons in the past. This methodology involves an excitation of one electron by a single-photon absorption out of collective states, which can be affected by energy fluctuations. In this project, NPL developed semiconductor detectors based on a single-electron quantum dot (a quantum dot that contains only one electron). Such a device would simplify the detection scheme, and a narrow-band, frequency-selective detection becomes possible.

Our proposed scheme for the realisation of single-photon detectors that covers this higher microwave-frequency range is to prepare one (and only one) electron in the ground state of a quantum dot. The ground state is isolated from the reservoir outside so the electron will stay in the dot for a relatively long duration. On the other hand, we prepared a tunnel barrier so that the first excited state is strongly coupled to the reservoir. If the electron absorbs a photon with the energy that matches the energy difference between the ground and excited states (excitation energy), the electron will be excited to the first excited state and it will tunnel out of the dot. This depopulation of an electron is monitored by a charge sensor placed next to the quantum dot, and is interpreted as a single-photon detection.

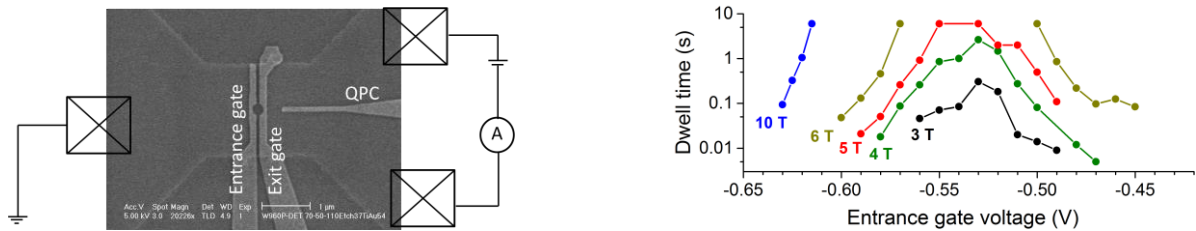


Figure 3.1.2.1. (a) Scanning-electron-microscope image and measurement circuit of a gallium-arsenide quantum-dot based detector. (b) The dependence of the electron dwell time on the entrance gate voltage and the applied magnetic field.

Figure 3.1.2.1a shows an image of a gallium-arsenide (GaAs) quantum-dot detector taken by a scanning electron microscope, and a schematic of the measurement circuit used for microwave photon detection. Two surface gates labelled as “Entrance gate” and “Exit gate” define a quantum dot under a circular cut out in the middle. A fast pulse voltage sequence applied to the entrance gate captures electrons into the quantum dot. The number of electrons and the dwell time of trapped electrons (the duration that electrons stay in the dot) can be tuned by the gate voltages and the external magnetic field applied to the device. The number of electrons in the quantum dot is monitored by the measurements of the current through a quantum point contact (a narrow channel) placed next to the dot by the gate labelled as “QPC” in the figure. In order for correct device operation, choosing the right set of design parameters, such as the size of the quantum dot, the position of the QPC detector, or its distance to the quantum dot, is important. During this project, we fabricated well over 20 devices with different designs and chose a couple of devices for microwave photon detection through device screening.

For microwave photon detection, firstly, we needed to verify that we can hold an electron long enough in the ground state of the dot. The electron dwell time is measured by repeating a number of cycles (typically 500), where in each cycle the time it took for the electron to escape the quantum dot is measured. One dataset of NPL’s dwell-time measurements is plotted in Figure 3.1.2.1b. This demonstrates that the electron dwell time can be tuned between a few milliseconds to ~ 10 seconds by varying the magnetic field and gate voltage. The lower limit is given by the time resolution of the detector current measurements. The upper limit is given by the limit set for the length of measurements (repeating longer measurements ~ 500 times would take too much time). The extrapolation of the line implies that the dwell time can be set at many hours, or even days.

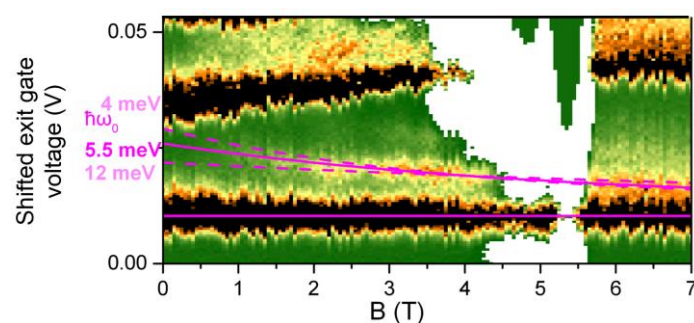


Figure 3.1.2.2. Excitation energy measurement. The change in the excitation energy is represented by the solid magenta line.

Another device characterisation that we needed to perform was the measurement of the excitation energy gap, as this affects the range of frequencies that our devices can detect microwave photons. NPL determined the excitation energy by measuring the excitation spectrum in the single-electron-transfer current. When electrons are excited into an excited state, they can tunnel back to the source reservoir while those in the ground state will stay in the dot and are transferred to the drain reservoir. This spectrum is shown in Figure 3.1.2.2, and the magenta line, a fitting curve to the Fock-Darwin model, gives an estimate of the quantum dot confinement energy of ~ 5 meV. The extrapolation of this line to the higher magnetic field suggests that at $B = 14$ T, the excitation gap corresponds to ~ 200 GHz photon excitation, which was close to the frequency of our many photon source (~ 180 GHz) used in the photon detection experiments.

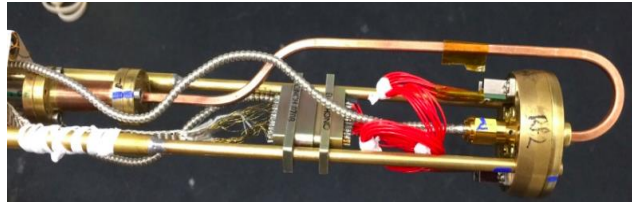


Figure 3.1.2.3. NPL's experimental setup for microwave photon detection using a semiconductor quantum dot. This shows a 180 GHz waveguide run from the top of the experimental probe to the sample holder (on the right), in which a quantum dot detector is mounted.

In order to perform microwave photon-detection experiments, NPL built an insert probe for their helium-3 cryostat with a 180 GHz waveguide running from the top of the insert (at room temperature) to the sample holder at the bottom (see Figure 3.1.2.3). The end of the waveguide opens directly above the chip with a quantum-dot detector (with ~ 1 mm distance). Although NPL expected a heavy attenuation (~ 30 dB or more) due to the length of the waveguide, a transmission test suggested that at least some photons reached the sample holder (the signal was too weak to measure this quantitatively). A combination of a Gunn diode and a frequency doubler was mounted on top of the probe as a many-photon source at 180 GHz.

The measurement protocol for single-photon detection is as follows. The quantum dot is loaded with one electron and the barrier is set so that the dwell time is about 10 seconds. One second after the electron loading, a pulse bias voltage is sent to the Gunn diode to radiate the chip with many photons for the duration of a few hundred milliseconds to a few seconds. An electron depopulation signal that coincides with the burst of microwave radiation is then looked for.

NPL attempted single-photon detection following the above procedure with a range of parameters (gate voltage setting, photon burst duration, etc.), but they were unable to find electron depopulation signals that consistently coincided with photon radiation pulses. Due to the limited resources (especially the measurement time in the cryostat), there is a large parameter space (magnetic field, gate voltages, etc.) that NPL were not able to search. There is still a possibility that this detector scheme would work under different conditions. However, within the parameter space that was searched, the conclusion is that the detection efficiency is zero.

NPL planned to integrate a niobium-based thermal photon source or Josephson junction source onto the chip as a collaboration activity between project partners, but they were unable to do this due to the delay in the development of the niobium fabrication on the GaAs substrate.

3.1.3 SNS detectors

For the frequency range from below 10 GHz up to about 80 GHz, the group at Aalto University, in collaboration with groups from Lancaster University (LanU) and INRIM, developed thermal detectors that comprised of superconductor - normal-metal - superconductor (SNS) nanostructures. Perhaps the most notable long-term application for this technology would be the development of a large-scale quantum computer based on microwave photon qubits. Other more immediate applications include ultrasensitive spectrum analysis in cryogenic environments: an area that is rapidly expanding for medical imaging, advanced sensing, cosmological observations and electrical metrology. A major advantage of thermal detectors compared to e.g. qubit-based detectors is that they typically present a suitable real input impedance for absorbing photons efficiently over a wide bandwidth and a large dynamic range. The natural drawback is that the temperature rise resulting from single-photon absorption is small, at most a few mK for microwave photons, therefore making its single-shot detection challenging. Our design exploits the sensitive temperature dependence of the impedance of nanowires that are under proximity-induced superconductivity. The devices developed in MICROPHOTON transduce the energy packet of a microwave pulse into a measurable electrical signal that can be detected with a radiofrequency probe, as the incoming microwave radiation modulates the electrical impedance of the SNS nanostructures.

Different types of SNS detectors were developed in close collaboration between Aalto, LanU, and INRIM. Initially, power sensors were fabricated and characterised, where a Joule heating effect was substituted for

the actual microwave input power in order to establish a calibrated device and proof of concept. Noise-equivalent power (NEP) below 10^{-16} W/Hz^{1/2} was demonstrated for an input power of 1 fW at 10 ms integration time. The second step was to develop a bolometer based on SNS junctions that is sensitive to a constant microwave heating power. With such a device, a NEP of about 10^{-17} W/Hz^{1/2} was demonstrated in microwave experiments. Finally, a ‘calorimeter’ sensitive to individual microwave energy packets was realized. These results lay the foundation for ultrasensitive microwave bolometry and calorimetry and, ultimately, single-photon detection.

Different approaches were tried in order to reach the single microwave energy quanta level sensitivity. One approach led by INRIM included fabrication of suspended normal-metal nanowires. The motivating hypothesis was that the suspension of the normal-metal nanowires would diminish the heat conductance between the detector and its environment in order to suppress energy fluctuation and the increase the detector’s thermal time constant. The fabrication process involves sputter deposition of high-quality superconducting and normal-metal thin films in the same vacuum chamber and then executing a state of the art three-dimensional nanopatterning process that includes a combination of electron beam lithography and directional focused ion-beam etching.

These devices turned out to have a low fabrication yield so a more traditional approach, based on electron beam lithography, was implemented immediately by LanU and Aalto. These devices were fabricated in two separate lithography steps and clean superconductor - normal-metal contacts were established by using Ar ion etching of the normal-metal nanowires prior to deposition of the superconducting leads.

In LanU’s version of this approach, a microwave resonator was damped by a normal-metal inclusion. Microwave power heated up the normal-metal and further damped the resonance causing a decrease in the quality factor of the device. In practice the integration of normal-metal components into the superconducting circuits was too demanding and the fabrication yield was also low.

One of the most productive approaches was the realisation of an SNS detector at Aalto. This device is shown in Figure 3.1.3.1. The device transduces a weak energy pulse into a radio-frequency electrical signal by reading out the modulation of temperature-dependent impedance in a proximised nanowire. This device achieved a resolution of approximately 200 microwave photons with a frequency of 8.4 GHz in a single shot, corresponding to an energy sensitivity of approximately 1.1 zJ, where $1 \text{ zJ} = 10^{-21} \text{ J}$ [13]. From these results there is a clear path toward single photon sensitivity by further reducing the heat capacity of the nanowire and using a state of the art quantum-limited amplifier at the readout. However, it should be noted that with regard to previous literature values on thermal radiation detectors, the measured sensitivity of about 1.1 zJ in this SNS-detector offers an order of magnitude improvement and goes beyond the former state of the art in this field. With further optimisation of the normal-metal photon absorber, sensitivity to single microwave energy quanta is in reach. The work completed in MICROPHOTON enables further improvements beyond the state of the art in microwave detection on a 1-2 year timescale.

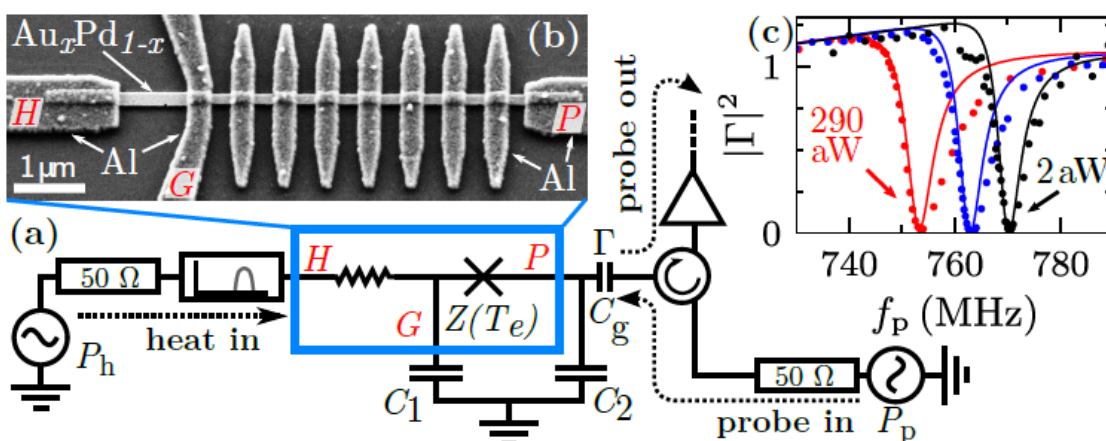


Figure 3.1.3.1. The SNS detector developed by Aalto [13]. (a) Circuit schematic indicating the input and readout. (b) Scanning electron micrograph of an actual device. (c) Measured signal in the bolometer operation mode demonstrating sensitivity to microwave power signals at the single attowatt level.

3.1.4 Bifurcation amplifier

A Josephson bifurcation amplifier (JBA) based on a Josephson junction or SQUID in a co-planar waveguide resonant cavity was first proposed by I. Siddiqi et al. in (2004).¹ Since that time, JBA has been widely applied for readout of the Josephson qubits. A sensitivity of about 10 microwave photons has been reached, but that requires signal averaging over many measurements. One aim of the MICROPHOTON project was to develop JBA towards single-photon sensitivity, but the main focus of the work on bifurcation amplifiers was experimental demonstration of period-doubling bifurcation (PDB) that had been predicted by Zorin and Makhlin in 2011.² The idea of the PDB detector (amplifier) for small microwave signals is based on using the nonlinear plasma resonance that can occur in a current-biased Josephson junction for parametric readout of Josephson qubits.

The work on “traditional” JBA was mainly performed by the group of Royal Holloway, University of London (RHUL). The first generation of combined JBA-PDB devices fabricated by PTB were used. However, that device was not fully compatible with the experimental setup of RHUL: very high RF powers needed to be injected, and that was incompatible with the refrigeration. Amplitude bifurcation was observed, but only near the half flux point. As a result, the bifurcation properties could not be fully mapped. Instead, a new feature was discovered in the studied sample. This was the instabilities in the flux modulation curve. This is probably due to the particular configuration of the RF SQUIDS and their interactions. NPL and RHUL are sensitive to this phenomenon for several reasons including our use of high Q-factor resonators. NPL and RHUL believe this serendipitous event to be some interesting and unexpected new physics of great relevance to the physics of SQUID arrays. They intend to explore this in future work. The work in the amplitude bifurcation regime was scientifically successful, but single-photon sensitivity could not yet be achieved.

In PDB work, the first task of the PTB and RHUL groups was to choose suitable nonlinear Josephson elements and to develop the optimum circuit layout. After several experiments with current-biased Josephson junctions (JJ) and current biased two-junction SQUIDS (dc SQUIDS), the PTB group came to the conclusion that the optimum design of the nonlinear element is a single non-hysteretic one-junction SQUID (i.e. RF-SQUID with a relatively low geometrical inductance, see Figure 3.1.4.1a), or a serial array of these components (Figure 3.1.4.1b). The magnetic control of the Josephson inductance and, more importantly, of its nonlinearity (including the possibility of completely suppressing quadratic or cubic nonlinearities on demand) was a great advantage of the circuits with embedded RF-SQUIDS.

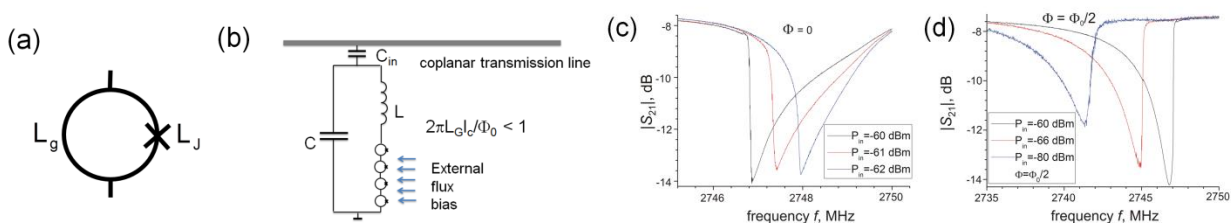


Figure 3.1.4.1. (a) Schematic of the RF-SQUID used as a basic nonlinear element. (b) A lumped-element resonance circuit including an array of RF-SQUIDS, which is capacitively coupled to a coplanar transmission line. (c) Left-turned nonlinear resonances in the superconducting circuit at a different drive power occurring due to the zero-flux-biased (generally, at $\Phi = n\Phi_0$, n is the integer) serial array of RF-SQUIDS having positive Kerr nonlinearity. (d) Right-turned resonance appearing in the same circuit at flux bias equal to $\Phi = (0.5 + n)\Phi_0$, corresponding to a negative value of the Kerr nonlinearity. In both (c) and (d) the quadratic nonlinearity vanishes. The resonance obtained at sufficiently large power exhibits characteristic bifurcations typical for a conventional JBA regime.

In the framework of MICROPHOTON PTB and RHUL have developed two types of PDB circuits, i.e. lumped-element (LE) circuits of a configuration shown schematically in Figure 3.1.4.1b and as a layout in Figure 3.1.4.2a and coplanar waveguide (CPW) based resonator circuits (see Figure 3.1.4.2b). The later samples which were also designed for transmission measurements included similar nonlinear elements which were embedded in the central conductor of the line (i.e. $\lambda/2$ resonator). For fabrication of these integrated circuits including JJs and resonators themselves, the multilayer Nb technology developed earlier at PTB was applied (see Figure 3.1.4.2c showing the cross-section of a JJ, and the figure caption).

¹ I. Siddiqi et al., Phys. Rev. Lett. 93, 207002 (2004)

² Zorin and Makhlin, PRB **83**, 224506 (2011)

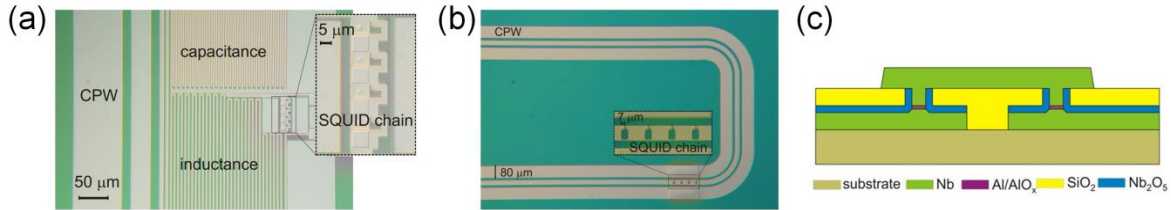


Figure 3.1.4.2. (a) Image of a fragment of a lumped-element resonator including an array of RF-SQUIDs. (b) Image of a fragment of a CPW-based $\lambda/2$ resonator including an array of RF-SQUIDs. (c) Cross-section (not to scale) of the Nb/Al/AIOx/Nb Josephson junctions ($j_c = 500 \text{ A/cm}^2$) after a chemical mechanical polishing (CMP) step (see details of the fabrication in [1] and R. Dolata et al.³).

Nb/Al/AIOx/Nb Josephson junctions were advantageous in their possibility to precisely characterise the junctions themselves as well as the nonlinear resonators, and to conduct primary measurements at a temperature of $T = 4.2 \text{ K}$. The cryogenic setup available at PTB allowed such measurement. The measurements at mK temperature were conducted at RHUL. Figure 3.1.4.3 shows the results of the measurement of the PDB sample at $T = 4.2 \text{ K}$. Due to a sufficiently large quality factor ($Q \sim 2000\text{-}3000$) and large quadratic nonlinearity, it was possible to achieve the PDB regime even in the case of a relatively low power of the pump signal delivered to the sample. An alternative strategy was to exploit the λ -resonance for the pump frequency in the same cavity. To do so, the groups of the SQUIDs had to be located at about 30 % and 70 % of the resonator length. For this design the nonlinear elements were located at the nodes of the currents in the standing waves of both the pump and the half of this tone and, therefore, this enabled the necessary mixing of the tones. The first observation of PDB at PTB was important progress beyond the state of the art in the field of microwave photon detection.

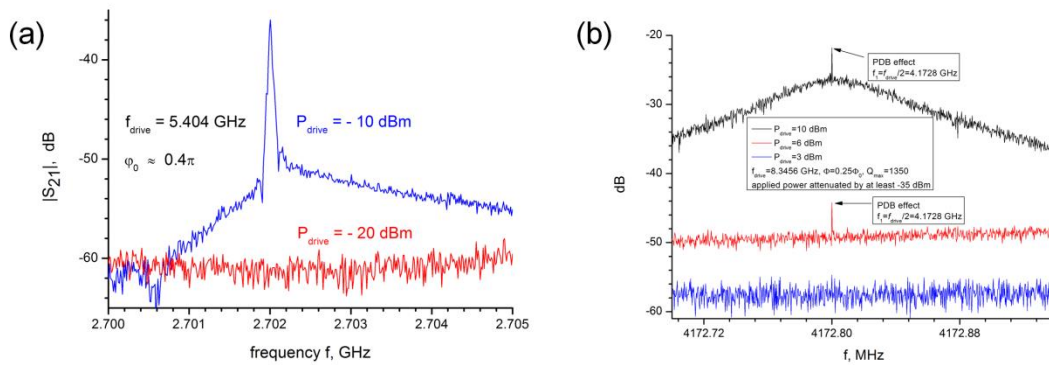


Figure 3.1.4.3. Excitation of the half tone frequency signal at the large pump due to quadratic nonlinearity in (a) the LE circuit and (b) CPW-based circuit both including short ($N = 4$) arrays of RF-SQUIDs. A dramatic increase of the background at a sufficiently large power of the pump is a fingerprint of the parametric amplification in the circuit.

PTB’s new design of the ‘universal amplifier’, which operates both in “traditional” JBA and PDB regimes, was cooled to $\approx 10 \text{ mK}$ at RHUL on a dilution refrigerator. RHUL has confirmed observation of the period doubling bifurcation phenomenon in this device and completed extensive measurements characterising the behaviour of the PDB. The device may be readily tuned between the JBA and PDB regimes by application of a magnetic flux. RHUL’s experiments also included exploring the device operation using pulsed microwaves. These measurements provided cumulative probability curves that will be helpful to guide the choice of parameters required to optimise future sample designs. They also experimentally demonstrated that there are two PDB stable points that may be chosen by controlling the phase of a microwave tone in the signal channel. The results show that PDB is sensitive and phase-sensitive to a microwave signal, but it was not yet possible to quantify the number of photons to which it is sensitive.

³ R. Dolata et al., J. Appl. Phys. 97, 054501 (2005)

In summary, the partners have developed the circuit design and improved the fabrication technology for superconducting resonator circuits with Josephson junctions and, most importantly, demonstrated the period-doubling bifurcation effect for the first time. The results show the potential of PDB as a detector of weak microwave signals. The results obtained have stimulated further development of cryogenic amplifiers/detectors operating in different regimes. In particular, the partners have proposed a traveling wave parametric amplifier with quadratic Josephson nonlinearity operating on the three-wave principle [15], which may potentially demonstrate a quantum-limited operation and this will likely outperform state-of-the-art counterpart parametric amplifiers with four-wave mixing.

3.1.5 Summary of microwave photon detectors

In summary, several versions of ultrasensitive cryogenic microwave detectors have been studied and developed towards single-photon sensitivity. Even though single-photon sensitivity with good fidelity could not be demonstrated during the lifetime of the project, there has been remarkable progress beyond the state-of-the-art towards that goal. With the SINIS single-electron trap detector it is already possible to observe events caused by individual microwave photons, but with a very small quantum efficiency. Such detectors can be applied, for example, to obtain spectral information on the microwave radiation penetrating quantum devices. With the SNS detector, the state-of-the-art of microwave photon detection sensitivity of thermal detectors was improved by more than an order of magnitude, to about 200 photons at 8.4 GHz frequency, and reaching single-photon sensitivity is feasible. A special property of thermal detectors is that they typically have a wide bandwidth and a large dynamic range. Operation of a new type of superconducting bifurcation amplifier, a period-doubling bifurcation (PDB) amplifier, was demonstrated for the first time. PDB detectors are expected to have better tuneability than amplitude bifurcation amplifiers, without compromising the feasibility of single-photon sensitivity.

3.2 ***Objective 2: Development of cryogenic sources of microwave photons to cover frequencies between 4 GHz and 300 GHz – a single-photon source based on a superconducting qubit, and other microwave photon sources based on biased Josephson junctions and on black-body radiation – and their use in the characterisation of the developed photon detectors.***

The second objective of the project required different solutions to be developed for microwave photon detection. For frequencies below 20 GHz, two types of quantum coherent on-demand single-photon sources based on superconducting qubits were developed. One of them is based on a transmon qubit coupled to a resonator with a resonance frequency between about 5 GHz and 10 GHz, and the other one is a unique tuneable source based on a tuneable gap flux qubit, connected to a long transmission line. More classical microwave photon sources were developed for higher frequencies: a Josephson junction photon source based on the microwave emission from a voltage-biased Josephson junction, and a thermal source based on the blackbody radiation from a heated normal-metal block inside a superconducting resonator. The final objective was to couple at least some of the developed sources with some of the detectors for mutual characterisation.

3.2.1 Single-photon source based on a superconducting transmon qubit

A superconducting qubit is in many ways the quintessential two-level system and the underlying physics can be understood by thinking of the qubit as a controllable 'artificial atom'. When sufficiently insulated from the environment the qubit will have two energy levels: a ground state $|0\rangle$ and an excited state $|1\rangle$. An excited qubit can - analogously to 'natural' atoms - relax back to its ground state by emitting a photon and superconducting qubits are engineered so that this energy difference corresponds to a photon with a frequency of a few GHz. Hence, we can create a single microwave photon source by implementing a circuit which allows us to first excite the qubit using e.g. a gate terminal and then controllably de-excite it into a microwave transmission line. This task is made easier if a high-Q microwave resonator is introduced, this serves both as a short term 'memory' and as a way to read-out and control the qubit.

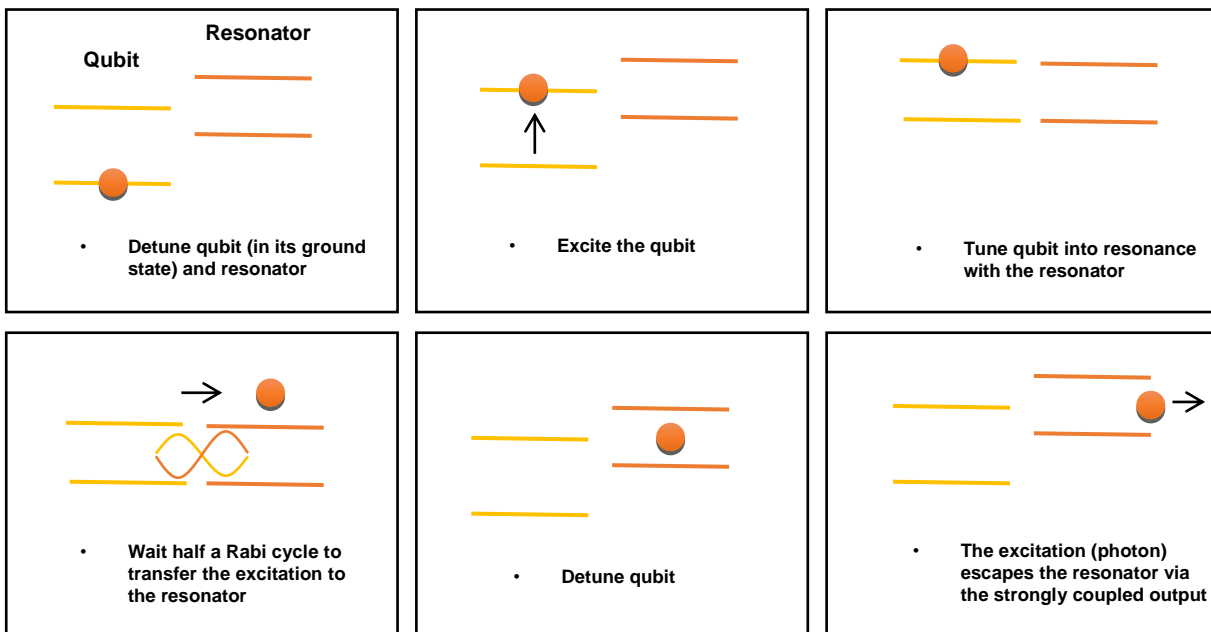


Figure 3.2.1.1. Operation principle of the on-demand microwave single-photon source.

There are several ways to implement a photon source using this so-called circuit-quantum electrodynamics (cQED) architecture. Figure 3.2.1.1 shows the most straightforward way to accomplish this. As can be seen several parameters come into play, most importantly the coherence time of the qubit and the resonator but also the strength of the coupling g between the qubit and the resonator. The timescale is set by how quickly the partners can tune the qubit (which is done by an applied magnetic field) and by g , the latter determining how quickly the excitation can be transferred from the qubit to the resonator.

Previous work in this context had primarily been done in relation to quantum computing and had not been focused on developing a practical source per se. The main objective in this project was to use this basic concept and develop an on-demand source that was *useful*, in this context. This means a triggered source (emitting precisely one photon when triggered by an electric pulse) with high efficiency (i.e. which has a high probability to emit a photon when triggered). The source also needs to be able to emit photons with a rate high enough for practical applications (typically about 10^6 photons per second). The latter requirement means that the choice of parameters will always be a compromise as the emission rate via the resonator γ_{κ} sets an upper limit on the quality factor of the resonator ($\propto 1/\gamma_{\kappa}$), but if the quality factor is too low the systems will be difficult to control and the emission efficiency will drop sharply. This means that very precise control over the parameters is necessary.

The design used went through several iterations and two full designs (henceforth referred to as MkI and MkII) were fabricated and later measured. The first batch (MkI design) was fabricated by staff from NPL and LanU using facilities at the MC2 cleanroom at Chalmers University of Technology (Sweden). Samples from this batch were subsequently measured at NPL and at LanU.

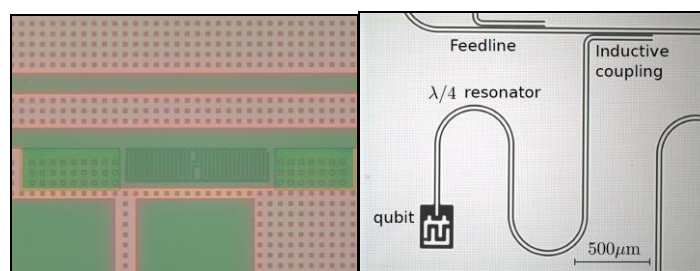


Figure 3.2.1.2. Micrographs showing parts of the MkI design (left) and MkII (right). The main difference between them is that MkI used a $\lambda/2$ resonator whereas the MkII design used multiplexed $\lambda/4$ resonators. Both designs used so called transmon qubits.

Three chips from the Mkl design were measured using the NPL cryogenic quantum measurement system which comprises a dilution refrigerator (base temperature 10 mK) equipped with state-of-the-art cryogenic high-electron-mobility transistor (HEMT) amplifiers, cryogenic isolators etc.; as well as associated microwave equipment.

Table 3.2.1.1. Designed and measured parameters for selected Mkl and MkII samples.

Design	Mkl Chip 1	Mkl Chip 3	MkII sample 1			
Resonator frequency	6 GHz (Mkl) 7.5 GHz (MkII)	5.94 GHz	5.94 GHz	7.52 GHz		
Resonator Quality factor		4000	2000	5400		
Qubit frequency	7 GHz	5.45 GHz	x	6.24 GHz	6.9 GHz	8.5 GHz
Qubit T1	1 μ s	40 ns	x	39 ns	x	4.7 μ s
Qubit T2	0.5 μ s	12 ns	x	20 ns	x	6.7 μ s (echo)
Qubit-resonator coupling	100 MHz	40 MHz	x	30 MHz	x	54 MHz

The static characterisation was done using a combination of two-tone spectroscopy and direct measurements of the transmission coefficient S_{21} of the resonator. The coherence time T_1 and dephasing time T_2 were measured directly using pulsed measurement to detecting Rabi oscillations and Hahn echoes, respectively.

The table above illustrates the problem with the Mkl design. Whereas the samples were working, the coherence times of the qubits were too small and the qubit-resonator coupling was also found to be too low. The very short T_1 means that the scheme outlined in Figure 3.2.1.1 could not be implemented. As an alternative a „static“ scheme where the qubit is not dynamically tuned was tested; this scheme could still result in a source with a theoretical efficiency of about 40 %. However, using the above parameters we can estimate the parameters of this system when operated using the static scheme. The emission rate $(g/\Delta)^2\kappa = 31$ kHz is too low to be detectable (peak power of -160 dBm) with conventional cryogenic amplifiers. The very short T_1 also implies that the qubit decays not via the resonator, but via some other mechanism meaning that most of the energy is lost to e.g. the dielectric and the polarisation was at best 75 %. The estimated efficiency was therefore only about $\gamma_{\kappa}/(1/T_1+2/T_2) \times 0.75 = 0.02$ %, and as a result photon emission could not be detected.

The MkII design addressed several of these issues. The key changes introduced in the design are: larger qubit level spacing, stronger qubit-resonator coupling. Another important modification of the design was the use of a multiplexing approach which, in principle, allows characterisation of 8 photon sources in one cooldown thus mitigating the chances of failure. This was achieved by using eight $\lambda/4$ resonators inductively coupled to a common feedline. Each transmon qubit is coupled capacitively to the resonator and located next to the end of the resonator centre line (see Figure 3.2.1.2 right).

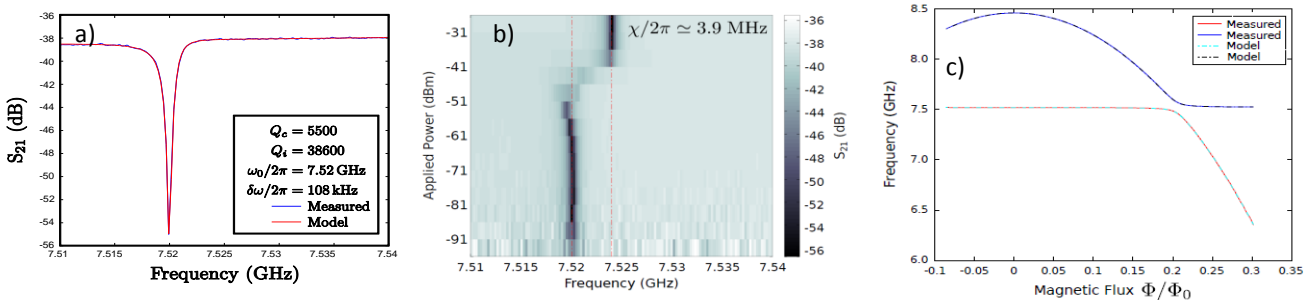


Figure 3.2.1.3. a) S_{21} vs. frequency for one of the $\lambda/4$ resonators measured through a feedline; b) S_{21} as a function of CW frequency and microwave power showing a shift of the resonator frequency due to the coupling to the qubit; c) Hybridisation between the resonator and the qubit measured by two microwave tone experiment, with one frequency probing the resonator around $\omega_r/2\pi = 7.52$ GHz, and a second probe tone following the qubit transition $\omega_a/2\pi$ controlled by an external magnetic flux.

The MkII design was fabricated in the Micronova cleanroom at Aalto University by staff from LanU and Aalto. Sample characterisation was performed at Aalto and NPL with a contribution from LanU, using a technique similar to the one described above. The main improvement compared to the MkI samples (see Table 3.2.1.1) is the observed coherence time $T_1 = 4.72 \mu\text{s}$ (see Figure 3.2.1.4 left), which compares favourably with the relaxation times measured in experiments by other groups. The qubit dephasing time was measured using the echo technique to eliminate low-frequency noise (see Figure 3.2.1.4 right). The coherent qubit evolution has $T_2 = 6.69 \mu\text{s}$ which is again similar to the state-of-the-art. The qubit-resonator coupling of 54 MHz also exceeds the requirements. This means that it should be possible to use the full dynamic scheme for photon generation.

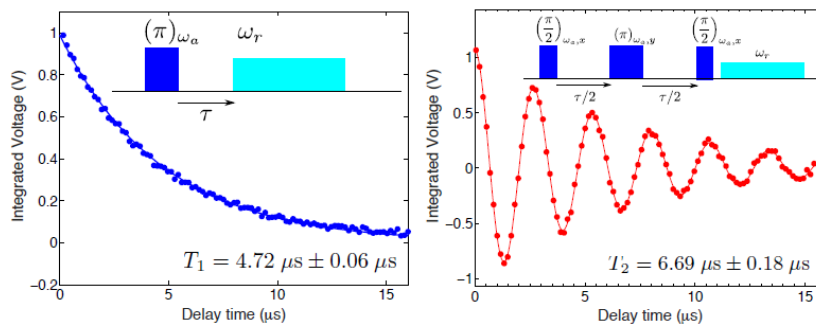


Figure 3.2.1.4. Measurement of the qubit characteristic coherence times. Left: The energy relaxation time of the qubit measured at the ‘sweet spot’. The exponential fit to the data gives $T_1 = 4.72 \pm 0.06 \mu\text{s}$. Right: Coherent evolution of the qubit with the echo technique applied. The fit to the data gives a dephasing time of $T_{2\text{echo}} = 6.69 \pm 0.18 \mu\text{s}$. Insets show the pulse sequence used to record the characteristic times.

Based on the measurement of MkII, we conclude that this second generation of samples was successful in terms of suitability as microwave single-photon sources. Firstly, we note that the resonators’ frequencies and quality factors were close to the designed ones. Secondly, the qubit parameters, such as the maximal energy gap which exceeds the resonator frequency by about 1 GHz, are also close to the desired ones. Third, the qubit-resonator and resonator-feedline couplings were consistent with expectations.

NPL has built up the capability to do correlation measurements of sources to verify their operation as single photon sources. Unfortunately, whereas the MkII design was promising, measurements of $g(1)$ or $g(2)$, were not possible. Measurements of this type have been done using the same system with the source from RHUL (Section 3.2.2).

3.2.2 Tuneable single-photon source based on a tuneable gap flux qubit

A limitation of the transmon qubit based single-photon source is that the frequency of the generated photons is fixed to that of the resonator of the circuit. That limitation is relaxed in another variation of an on-demand microwave photon source based on a superconducting tuneable gap flux qubit used as an artificial atom. In that device, the artificial atom is connected to a long transmission line instead of a resonator, and the frequency of the generated photons can be tuned in a wide range, from 6.7 GHz to 9.1 GHz. The operation of the device as a tuneable on-demand single-photon source has been successfully demonstrated, and the results of this work have been published in Nature Communications [14].

The work has been done by the RHUL group in collaboration with NPL and RIKEN (Tsukuba, Japan). Within the project, several designs of the device have been investigated and analysed at RHUL. The device elements have been characterised at RHUL and NPL. The first quantum systems – superconducting two-level systems coupled to a transmission line – have been measured at NPL and RHUL. The initial characterisation of the photon source has been performed by a RHUL postdoc on the equipment of RIKEN. Next generations of the devices have also been studied at NPL. To provide a solid proof of the photon source operation, the second-order correlation function has been studied by the RHUL postdoc on the RIKEN equipment and at NPL. The photon source is planned to be combined with a microwave photon detector developed in Aalto, but that work is extended beyond the MICROPHOTON project due to its complexity.

The idea of the single-photon source is based on the fundamental quantum-optical effect of spontaneous emission from an excited two-level atom. An optical analogue of the single-photon source consists of a two-level atom situated near a tiny hole (much smaller than the wavelength) in a non-transparent screen (Figure 3.2.2.1a). The atom is slightly shifted towards the right-hand-side space, defining an asymmetric coupling to the half-spaces. By applying a powerful pulse of light from the left side, the atom can be excited by evanescent waves, which cannot propagate in the right-hand-side space due to their rapid decay. On the other hand, the excited atom emits photons into the right-hand-side space (Fig 3.2.2.1b). In practice, the presented layout is difficult to build using natural atoms and, even if one succeeds, another problem must be solved: the low collection efficiency of emitted photons in the 3D space.

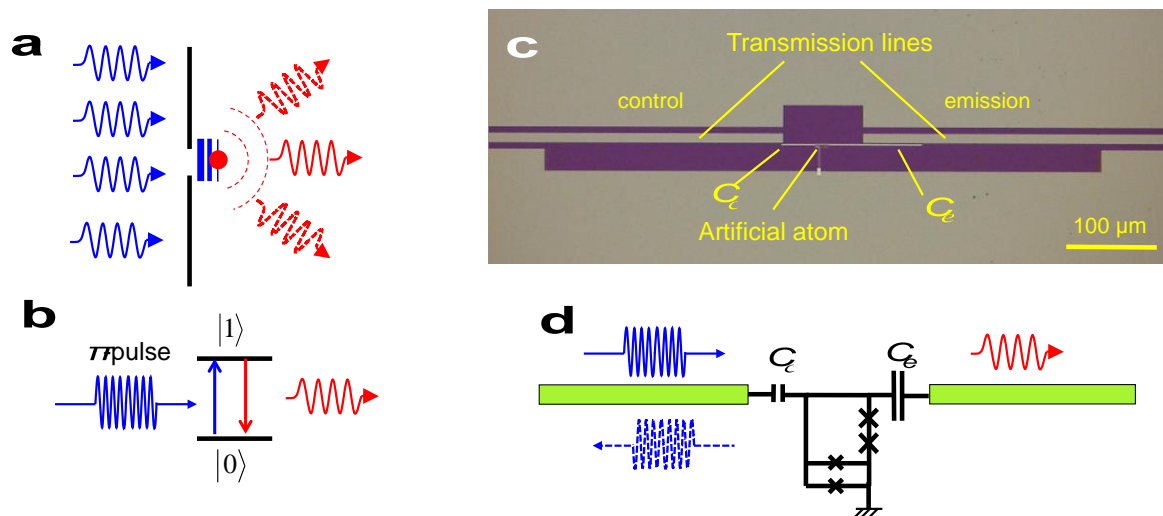


Figure 3.2.2.1. The tuneable on-demand single-photon source. a) Optical analogue of the source. A non-transparent screen with a hole, much less than a wavelength, forms two half-spaces. A two-level atom is situated in the right subspace close to the hole. The incident light from the left-hand side excites the atom by evanescent waves, which, however, cannot penetrate through the hole. The excited atom, in turn, emits radiation mainly into the right sub-space. b) Mechanism of the single-photon generation. The atom excited by a π -pulse (blue) of the incident radiation relaxes with a photon emission into the right sub-space (denoted by red colour). c) Optical micrograph of the device. The artificial atom is in the middle and the thin long metallic line from the atomic loop forms capacitances between the atom and the control/emission transmission lines. d) An equivalent electrical circuit of the photon source. A superconducting loop with two junctions and an α -loop at the bottom forms the tuneable two-level quantum system.

These problems have been solved by using on-chip superconducting quantum circuits coupled to 1D transmission lines. Figure 3.2.2.1c shows a circuit with an artificial atom coupled asymmetrically to a pair of open-ended coplanar transmission lines (1D-half spaces), each with $Z = 50 \Omega$ impedance. The coupling capacitances C_c and C_r are between the artificial atom and the control and emission lines, respectively (shown on the equivalent circuit in Figure 3.2.2.1d). The capacitances can be approximated as point-like objects because their sizes are much smaller than the wavelength of the radiation ($\lambda \sim 1$ cm).

A microwave pulse is applied from the control line, exciting the atom, and then the atom emits a photon mainly to the emission line due to asymmetric coupling: $C_c/C_r \approx 30$. The following are intrinsic features of the device: The two lines are well isolated from each other so that the excitation pulse does not leak from the control line to the emission line; due to the strong asymmetry, the excited atom emits a photon with up to $1 - (C_c/C_r)^2$ output probability; the photon is confined in the 1D transmission line and can be easily delivered to other circuit elements through the line.

The artificial atom schematically shown in Figure 3.2.2.1d is a controllable two-level system based on a tuneable gap flux qubit that is coupled to two Nb coplanar lines. The atom is fabricated by Al/AIOx/Al shadow evaporation techniques. It contains two identical junctions in series implemented in the loop together with a dc-SQUID (called an α -loop), shown in the bottom part of the device in Figure 3.2.2.1d. The magnetic fluxes are quantised in the loop: an integer number, N , of the magnetic flux quanta, Φ_0 , can be trapped. At the

magnetic fields where the induced magnetic flux in the loop is equal to $\Phi = \Phi_0 (N+1/2)$, two adjacent flux states $|0\rangle$ and $|1\rangle$ with N and $N+1$ flux quanta, which corresponds to oppositely circulating persistent currents, are degenerate. The degeneracy is lifted due to the finite flux tunnelling energy ΔN , determined by the effective dc-SQUID Josephson energy and varies between different degeneracy points (depends on N). The energy splitting of the atom $\hbar\omega_{10}$ is controlled by fine adjustment of the magnetic field $\delta\Phi$ in the vicinity of the degeneracy points, where $\delta\Phi = \Phi - \Phi_0 (N+1/2)$, and I_p is the persistent current in the main loop.

Our photon source based on the conversion of an atomic excitation into a MW photon requires efficient control of the quantum states. Figure 3.2.2.2a shows measured quantum oscillations. The partners monitor the coherent emission from the atom into the emission line by VNA when a train of identical excitation MW pulses, each of length Δt with period $T = 80$ ns, is applied from the control line. The amplitude of the emission oscillates with Δt . The maxima and minima of the oscillations correspond to $|\langle\sigma^+\rangle| \approx 1$ and $|\langle\sigma^-\rangle| \approx 1$, when the atom is in the maximally superposed states with 50 % population.

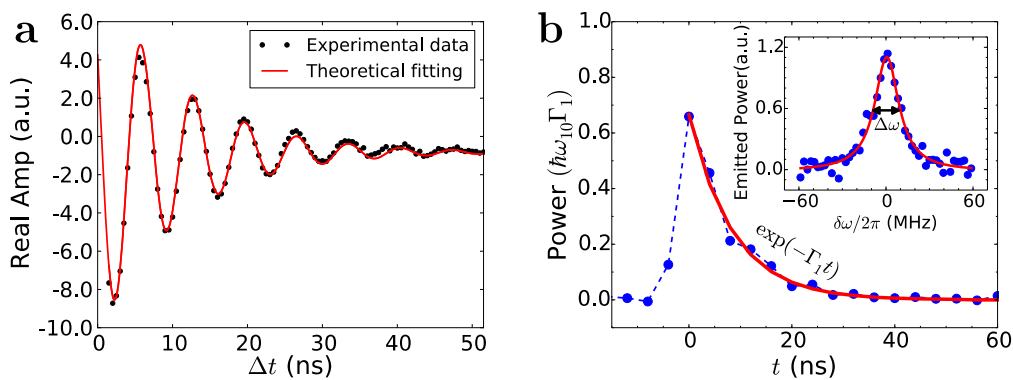


Figure 3.2.2.2. Device operation. a) Rabi oscillations of the two-level atom coupled to the two half-spaces measured by VNA. The atom is excited by MW pulses of length Δt from the control line with a repetition time of $T = 80$ ns, and the coherent emission is detected from the emission line. b) The emitted photon shape normalised to the single photon power. The red solid curve shows a fit to $\exp(-\Gamma_1 t)$. The inset demonstrates an emission peak (blue dots), when a π -pulse is applied at Δt_π fitted by a red Lorentzian curve $\Delta\omega = \Gamma_1$.

For the single-photon source operation, the partners tune the pulse length to obtain the maximum incoherent emission (defined as a π -pulse and its length is $\Delta t_\pi = 3.5$ ns), emitting a single photon from the atom excited state in every pulse period. The traces are then amplified and digitised with a sampling time of 4 ns. The traces $V(t)$ of repeated measurements are then squared and accumulated. The typical photon shape $P(t)$ obtained after 2×10^9 times averaging is shown in Figure 3.2.2.2b. The inset shows the averaged emission power peak excited by the π -pulses with repetition time and measured by a spectrum analyser. Using a Lorentzian fit, the partners obtain a FWHM $\Delta\omega/2\pi \approx 20$ MHz, which is equal to the relaxation rate Γ_1 .

The two-level system operation together with the Rabi oscillations prove that the source generates a single photon at a time with a photon generation efficiency of at least 75 % and with a tuneable frequency between 6.7 GHz and 9.1 GHz. Nevertheless, the partners provide additional evidence of the single-photon generation by measuring the second-order correlation function with linear detectors (microwave amplifiers). Such a demonstration is straightforward in optics due to the existence of photon counters but this is extremely demanding in the microwave range, where the microwave amplifiers have a typical signal-to-noise ratio in the single-photon regime is less than 10^{-2} in power and, therefore, long accumulation of statistics which is required.

The circuit schematically shown in Figure 3.2.2.3a is implemented to perform Hanbury-Brown-Twiss measurements (HBT) using linear detectors. The partners accumulate traces each consisting of a train of 40 pulses with a period of $T = 160$ ns. The emitted photons are then transmitted through an isolator to a 90 degree hybrid coupler operating as a microwave beam splitter. The idle input port terminated by 50Ω is a source of vacuum noise. The two signals coming from the splitter output ports of the hybrid coupler are amplified by amplifiers at 4.2 K and at room temperature. The partners assume that the noise added by the amplifiers are uncorrelated in each channel. Next, the signals, down-converted to close to zero-frequency with mixers, are passed through 30 MHz bandwidth low-pass filters and voltage amplitudes $V_1(t)$ and $V_2(t)$

are recorded by two digitisers. Finally, the traces are read out and treated by a PC to extract the two-point correlation functions.

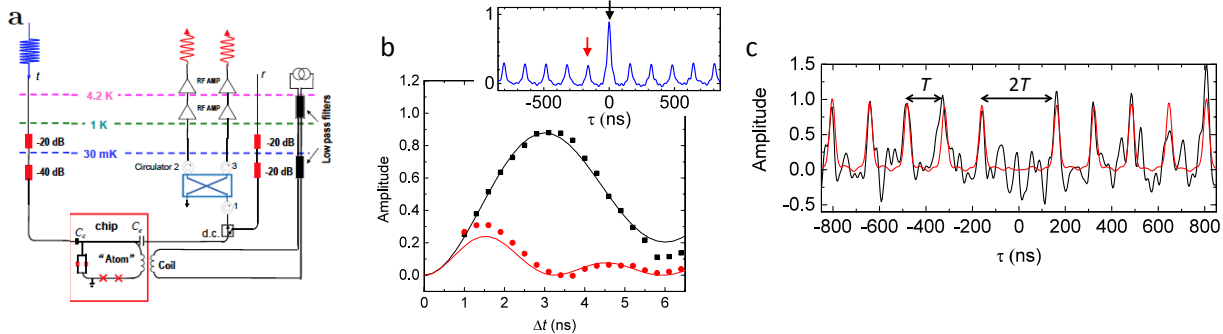


Figure 3.2.2.3. Correlation function measurements. a) The experimental setup for HBT measurements with linear detectors in the microwave frequency domain. b) The first-order correlation function dynamics. The inset shows typical $g^{(1)}(\tau)$. The black squares and red dots represent experimentally measured dynamics of the central peak $g^{(1)}(0)$ and side peaks $g^{(1)}(nT)$, respectively. The solid curves show simulations with the actual device parameters, including dissipation. c) The black curve is a measured second-order correlation function $g^{(2)}(\tau)$ and the red one represents the simulated second-order correlation function using the measured photon traces. The second-order correlation function is a result of averaging of 1.5×10^{10} traces with 1600 points in each trace with a 4 ns sampling rate. The curves are then additionally smoothed out.

First, the partners demonstrated the first-order correlation function $g^{(1)}(t) = \int V_1(t) V_2(t+t) dt$ of the two signals. The normalised function with subtracted background is exemplified in an inset of Figure 3.2.2.3b. The central peak $g^{(1)}(0)$ corresponds to the total power emitted by the atom and the side peaks $g^{(1)}(nT)$ correspond to the coherent emission. The dynamics of the peaks as a function of the excitation pulse length is shown in Figure 3.2.2.3b. The solid lines demonstrate simulations with the previously extracted device parameters.

Next, the partners calculated the second order correlated function of the emitted radiation defined as $g^{(2)}(t) = \int |V_1(t)|^2 |V_2(t+t)|^2 dt$. The result of $g^{(2)}(\tau)$ measurements after averaging of 1.5×10^{10} traces is shown in Figure 3.2.2.3c. The traces are additionally smoothed to reduce fluctuations. The red curves show expectations calculated with the measured photon shapes. We observe a series of side peaks spaced by T with a suppressed peak at zero delay time $\tau = 0$. The observed anti-bunching of the emission demonstrates the single-photon generation.

3.2.3 Josephson junction photon source

For the purpose of calibration of the SINIS detectors in the frequency range between about 50 GHz and 200 GHz, PTB optimised the layout and fabricated an on-chip microwave generator based on the well-known Josephson generation phenomenon. The advantages of the selected approach are as follows:

- Under certain conditions, the Josephson junction can produce an almost monochromatic voltage oscillating signal, with the higher harmonics being suppressed sufficiently strongly to be neglected in applications.
- Simple tuneability of the fundamental Josephson frequency by adjusting the average voltage across the junction. Furthermore, in the SQUID-layout [see Figure 3.2.3.1(b,c)] the amplitude of the oscillations can be tuned by magnetic flux through the SQUID loop.
- When designed in the same technology as the SINIS detector, the Josephson source can be conveniently co-fabricated on the same chip with the detector (see Section 3.1.1), thus minimising the signal losses between the source and detector.

Significant improvements were done at PTB to minimise on-chip heat generation, while maximising the amplitude of the generated signal. The standard dc shunt was not included in the design. Instead, four rf-shunts of a sufficiently large bulk volume were inserted, close to the Al/AlO_x/Al Josephson junctions, into the biasing leads, as shown in Figure 3.2.3.1a. For achieving an appropriate shunt resistivity a specially

developed Ti/AuPd (30 nm / 5 nm) bilayer was elaborated, with the high-ohmic Ti-film evaporated in the presence of oxygen. An important advantage of using the bilayer system (and not, for example, single-layer, AuPd-only elements) was a considerably larger shunt volume, which enabled more effective electron thermalisation in the shunt and lower electron temperatures, down to about 100 mK. This resulted in a smaller generation linewidth, at the level of a few GHz only. On the other hand, covering Ti with a thin layer of AuPd as a noble metal stopped further oxidation of Ti by the atmospheric oxygen and improved the galvanic contact to the upper layer of Al as the lead and junction material.

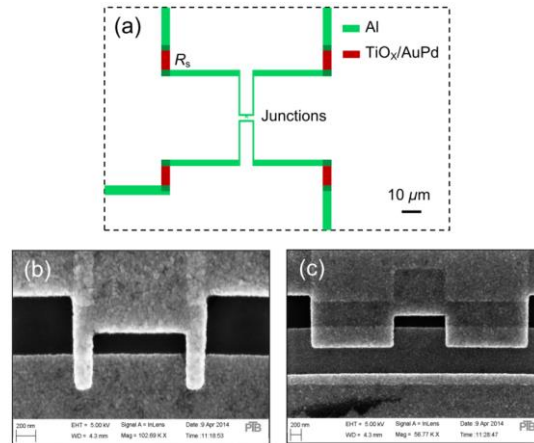


Figure 3.2.3.1. Layout sketch of the rf-shunted Josephson junction source of microwaves (a) and SEM pictures of the SQUID design with two different dimensions of the Josephson junctions used in experiments (b,c).

Tuneability of the microwave amplitude (and power) was achieved with the help of a SQUID layout of the Josephson source. The PTB group implemented several junctions of different areas as shown in Figure 3.2.3.1(b,c) and found a better magnetic controllability of the smaller devices which were later selected for the calibration experiment (see Section 3.2.5).

The devices were studied at mK-temperatures with respect to the stability of their dc operating point in a certain Josephson voltage and frequency range.⁴ The critical current values were measured for different junction areas. The results were brought together with the theoretical estimations of oscillation amplitude, see Figure 3.2.3.2, thus providing the first-iteration reference for the experiments summarised in Section 3.2.5.

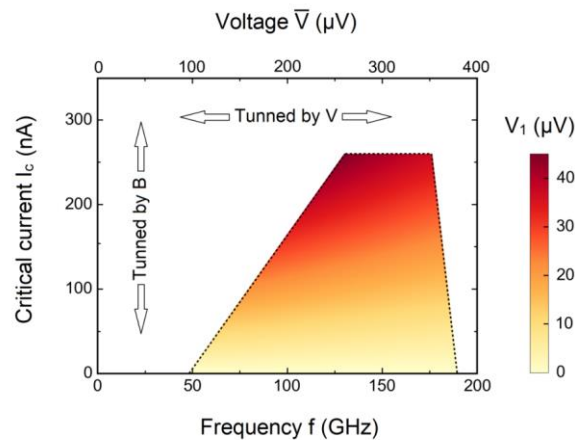


Figure 3.2.3.2. The amplitude profile of the Josephson oscillations (the fundamental harmonics) as a function of critical current and Josephson frequency (voltage).

⁴ B. Jalali-Jafari, S.V. Lotkhov, and A.B. Zorin, *Al/AIO_x/Al-Josephson-junction-based microwave generators for weak-signal applications below 100 mK*, arXiv:1410.5314 (2014).

INRIM developed technology for fabricating niobium-based Josephson junction devices on GaAs substrate. The purpose was to use the devices as microwave photon sources in the characterisation of semiconductor quantum dot detectors. After unsuccessful attempts with focused ion beam (FIB) techniques, INRIM moved to the SNIS multilayer technology based on the selective anodisation process through an electron beam lithography (EBL) defined mask on GaAs substrates covered by PECVD grown SiO_2 dielectric (see Figure 3.2.3.3). Characterisation results at 4.2 K have confirmed their agreement with the expected electrical parameters and their tuneability with sizes and the oxidation process.

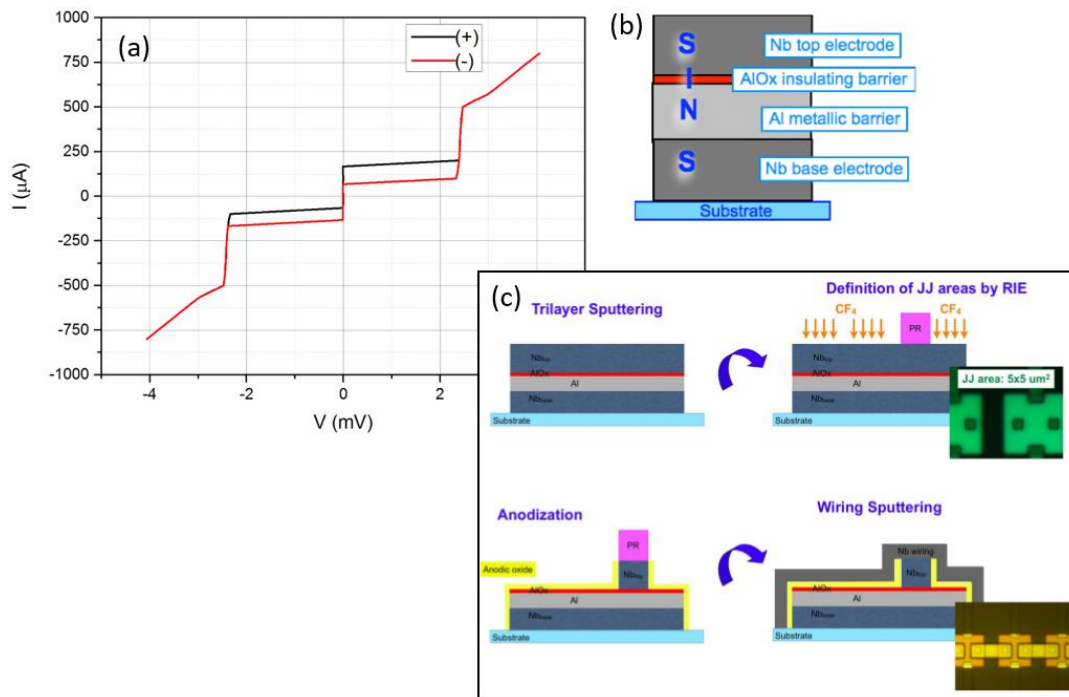


Figure 3.2.3.3. (a) The I - V characteristic of a $3.14 \mu\text{m}^2$ junction fabricated on a GaAs substrate covered by 200 nm of SiO_2 grown by PECVD. Measurements have been performed at $T=4.2$ K. Extrapolated $R_N = 4.5 \Omega$, $J_c = 5.2 \text{ kA/cm}^2$ and $V_{\text{Gap}}=2.4$ mV are in good agreement with typical SNIS parameters. (b) Sketch of the SNIS multilayer. (c) Scheme of the process implemented on a GaAs/ SiO_2 substrate.

3.2.4 Thermal photon source

Prior to the MICROPHOTON project, there have been only a few technologies capable of on-demand microwave output at the single-photon level, mostly based on superconducting quantum bits. The narrow scope of microwave photon sources has prevented extension of optical frequency photonics applications into the microwave regime, outside of a few specialised scenarios. Aalto, INRIM and NPL directly addressed this problem within the project.

The partners considered a potential solution to the lack of deterministic microwave photon sources by integrating normal-metal components into the framework of circuit quantum electrodynamics. The superconducting circuit elements act as low-loss carriers of microwave signals, while the normal-metal components behave as engineered dissipative elements and/or thermal reservoirs. One can understand the operation principle of the source in the following way. The normal-metal elements heat up under an electronic excitation and emit a blackbody spectrum at the characteristic temperature of a few hundred millikelvin. That gigahertz-frequency output spectrum can then be easily transported via the superconducting waveguides and sent off the chip to be boosted by commercial low-noise amplifiers.

The operation principle of the proposed thermal microwave photon source is that an input pump tone heats up a proximated normal-metal nanowire to a temperature that radiates microwave photons at the output waveguide. Thanks to the designed frequency separation between the pump and output, there is minimal leakage of unwanted microwave power to the output. In practice it was difficult to meet the fabrication challenges of engineering nanoscale normal-metal wires into superconducting circuits.

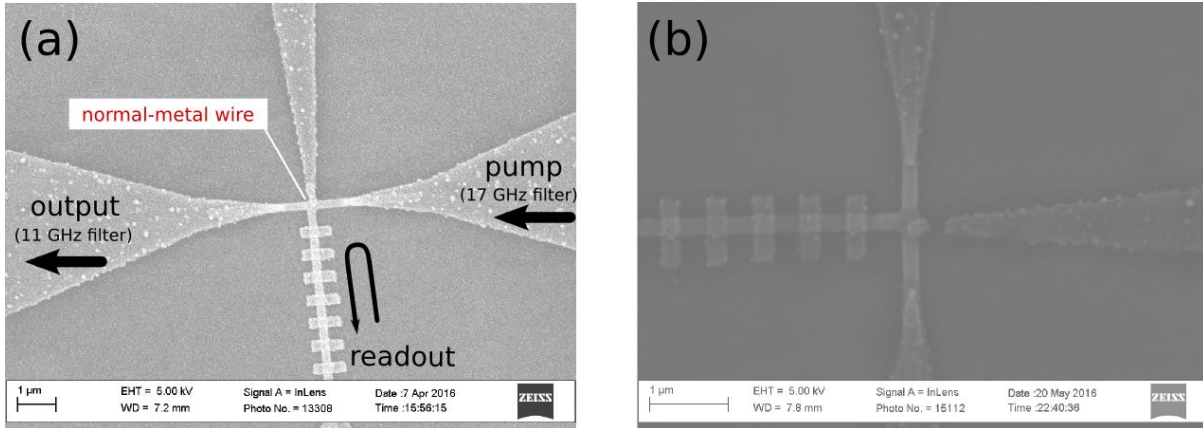


Figure 3.2.4.1. (a) A thermal photon source fabricated at INRIM that integrates normal-metal elements into a superconducting circuit. The normal-metal reservoir functions as an engineered dissipative element that produces an emission spectrum peaked at a few gigahertz corresponding to its characteristic temperature (at a few hundred millikelvin). Superconducting transmission line filters efficiently route the signal off the chip to a commercial low-noise amplifier. The readout line measures the characteristic temperature by probing a nanoscale resonant circuit. (b) The same device after the measurement. The discontinuity demolishes the expected operation.

The measurement was focused on revealing the normal-metal–superconductor detector sensitivity for environmental temperature change and microwave heating through the pump and the output filters. The junction was monitored using an auxiliary line, which consists of a superconductor-normal-metal-superconductor array, and two dielectric plates. In a cryogenic environment the array creates kinetic inductance. The value of the inductance increases with temperature. The absorbed photons heat up the reservoir, therefore causing a temperature change. The coupled LC oscillator detects photon absorption in this way.

First, the readout line's characteristic frequency has to be found. Systemically, the frequency peak in each device is higher than the nominal value. Though, thermal response is detectable. One successful calibration is depicted in Figure 3.2.4.2a. If this phase provided reasonable sensitivity, the characterisation can proceed.

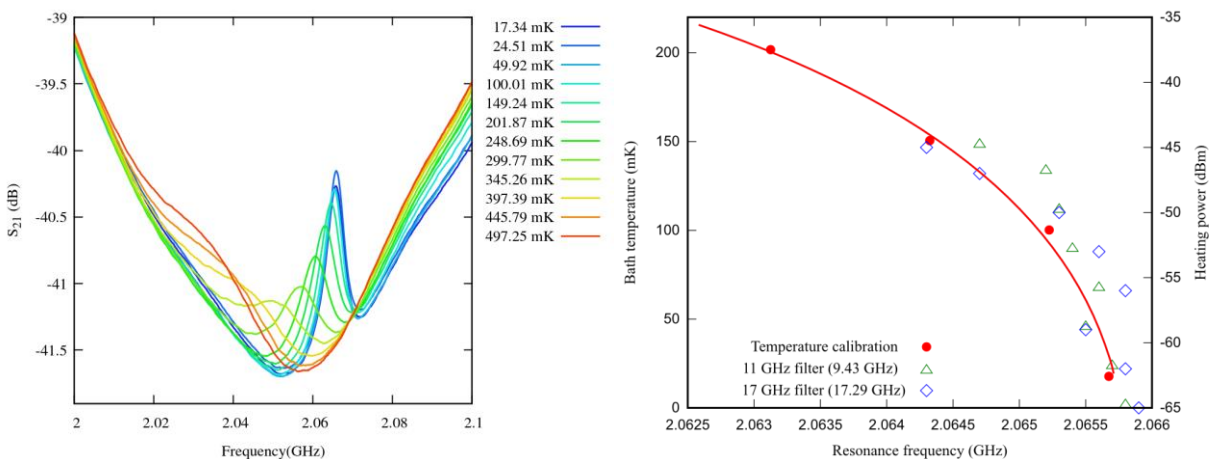


Figure 3.2.4.2. (a) A readout temperature calibration measurement. The bath temperature changes the readout circuit and the system responds at a different frequency. (b) Thermal calibration and microwave excitation comparison. The red points show the resonance shift due to changing bath temperature. The green and blue marks represent microwave heating on a 11 GHz and 17 GHz filter, respectively. It shows the effect of applying different heating powers.

In the next step using the results obtained, the junction temperature can be surveyed at any time. The output radiation is determined by the accurate measurement of the readout and of the environmental temperature. To characterise the pump and output channels the partners used heater pulses at the base temperature. The reservoir temperature was observed, and each excitation which caused heat absorption, was matched to an equivalent effect on the environmental temperature change. Figure 3.2.4.2b shows one example of matching thermalisation and in-resonance microwave heating. Although the applied microwave input heats the normal-metal junction, the power scale is much higher, which was designed.

A typical failure mode of the sources fabricated by INRIM was the non-continuity of the normal metal components, as shown in Figure 3.2.4.1b. The devices had a deviation in transmission line geometry, which is related to the fabrication process. This issue can be responsible for the normal metal reservoir's low microwave sensitivity. Additionally, this work stressed the need for high-quality dielectric material in the on-chip capacitors. Altogether five different thermal sources that were fabricated by INRIM were characterised by Aalto and/or NPL in separate cooldown cycles. None of these devices worked as designed.

However, these measurement results were important in the development of a new tunnel junction based source at Aalto that has been investigated after the end of the MICROPHOTON project. That design relies on the photon emission associated with electron tunnelling events in a nanoscale superconductor--insulator--normal-metal junction. It has turned out that when considering a detailed picture of the energetics of quantum tunnelling, microwave frequency radiation is emitted in a controllable way during electron tunnelling. This effect can be exploited to produce an on demand thermal photon source. Aalto has demonstrated that the thermal source based on tunnelling works efficiently, and has measured the output power and frequency with a spectrum analyser to match with simulations based on microscopic quantum theory. This source looks promising for integration with a detector since it heats up the resonator mode directly, as opposed to heating up the superconductor and creating quasiparticles. Therefore, the integrated resistor does not need to be at high temperature and does not lead to excess heating of quantum devices.

3.2.5 Josephson junction photon source coupled with SINIS and NISIN detectors

For the purposes of verification and calibration, the SINIS trap detector (see Section 3.1.1) was integrated on-chip with the Josephson SQUID based microwave source (see Section 3.2.3), within the circuit layout shown in Figure 3.2.5.1. The detector's response was measured as a function of microwave frequency and power. The result was compared with theoretical calculations of photon-assisted tunnelling (PAT) rates. Additionally, the contribution of the acoustic device coupling via substrate phonons generated by the Josephson source as a side product was evaluated in a dedicated layout including an uncoupled microwave source.

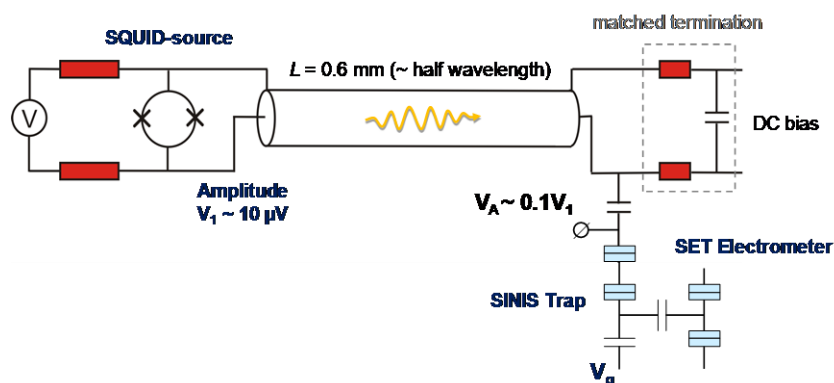


Figure 3.2.5.1. Equivalent circuit of the integral device of the PTB group, including the microwave SQUID source, a coplanar transmission line with an impedance-matched termination and the SINIS trap detector, all co-fabricated on the same chip.

A strong effect of the Josephson radiation was confirmed both on the depth of charge hysteresis, see Figure 3.2.5.2a, and on discrete charge dynamics of the trap, Figure 3.2.5.2b. This gives one more clear demonstration of the essentially quantum interaction of light (microwave signal) and matter (trapped electron) in the form of the photon-assisted tunnelling effect.

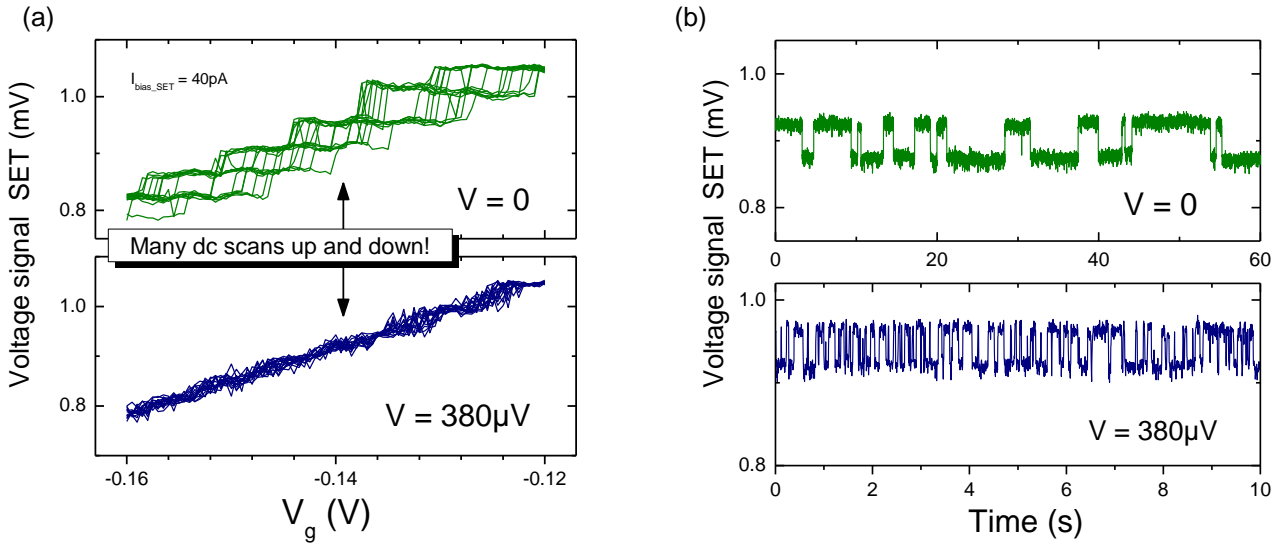


Figure 3.2.5.2. Charge hysteresis (a) and time track of electron hopping (b) in the SINIS trap without (Josephson voltage $V = 0$) and with irradiation ($V = 380 \mu\text{V}$). The charge state of the trap is read out by the capacitively coupled SET electrometer. V_g is a dc control voltage used for tuning the Coulomb barrier in the trap.

The PAT rate inferred from the state switching statistics was compared with theoretical predictions and both demonstrated a clear threshold-type operation of the SINIS detector, with the (tuneable) activation threshold around 100 GHz ($V \approx 200 \mu\text{V}$), see Figure 3.2.5.3. The data were used to calibrate the activation threshold (as well as, roughly, the microwave coupling coefficient) against the Josephson voltage as a first-principle frequency reference.

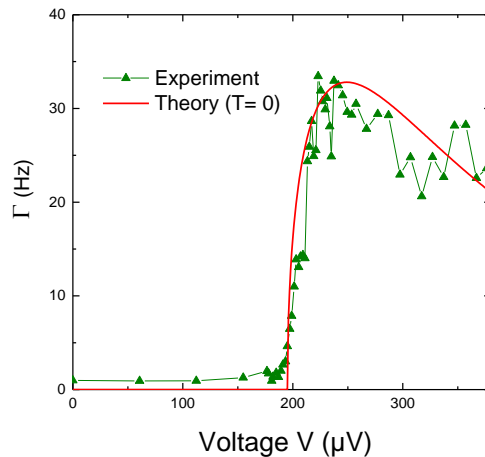


Figure 3.2.5.3. Calculated (solid line) and measured (symbols) PAT rates as a function of the Josephson voltage.

In a similar layout with the NISIN transistor as a detector, the effect of irradiation manifested itself in the suppression of the parity effect in the superconducting S-island. This process showed up as a periodicity change from $2e$ to $1e$, shown in Figure 3.2.5.4, as the microwave absorption helped to excite quasiparticles (and invoke the related detector current signal) even in the even-electron-number states with the strong Coulomb blockade.

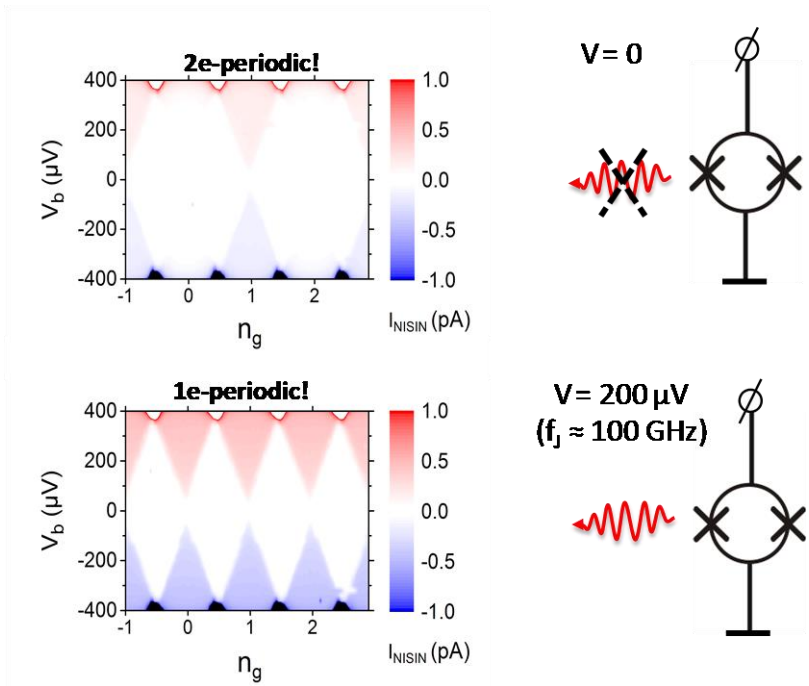


Figure 3.2.5.4. Microwave irradiation effect on the NISIN transistor detector. An originally low dc current signal I_{NISIN} in the detector raised up due to radiative excitation of quasiparticles, accompanied by suppression of $2e$ -periodicity of the current vs. number of electrons n_g in the superconducting island.

The NISIN and SISIS detector responses were found to be tuneable in a periodic manner by magnetic flux through the SQUID, see Figure 3.2.5.5a, which is a good confirmation of power tuneability of the SQUID microwave source. Similar to the SINIS trap, the detection curves exhibited a clear activation threshold (most pronounced in the case of the SISIS detector, the data is shown in Figure 3.2.5.5b) with respect to the microwave frequency f , being indicative of the photon energy hf . The transition width of the activation threshold in the SISIS detector was used to find an upper estimate for the generation linewidth of source, $\Delta f_D \sim 2$ GHz. This estimate is consistent with the theoretical evaluation of the thermally defined linewidth of the Josephson oscillations (see Section 3.2.3).

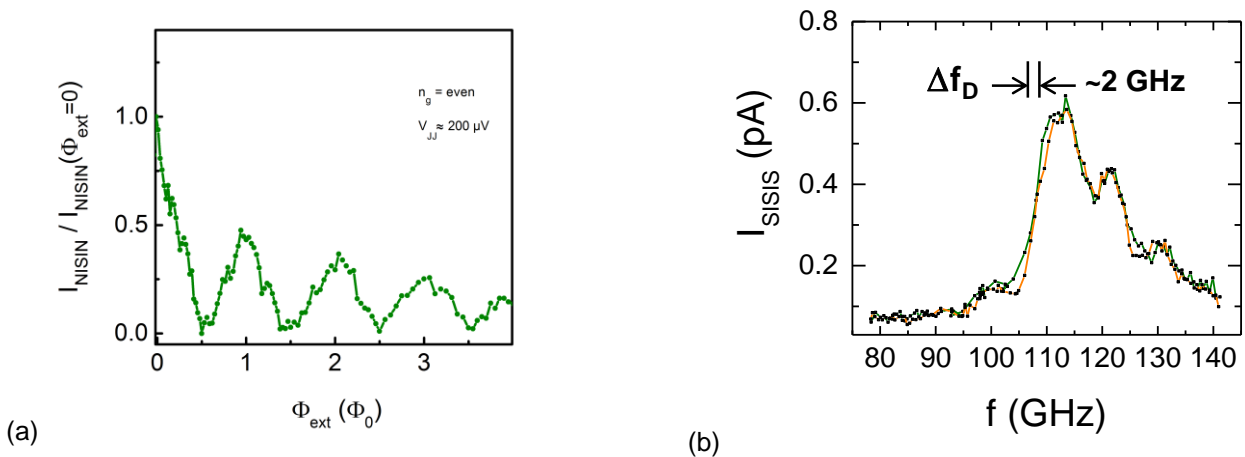


Figure 3.2.5.5. (a) Periodic dependence of the current signal of the NISIN detector on the flux through the SQUID expressed in units of a flux quantum $\Phi_0 \approx 2.07 \times 10^{-15}$ Wb. (b) Frequency dependence of the SISIS-detector current exhibiting a sharp threshold at the photon frequency $f \sim 100$ GHz.

In a further experiment with an additional electromagnetically-uncoupled Josephson source placed at the same distance to either SINIS or NISIN detector, PTB evaluated the input of acoustic phonons, produced by the Josephson source as a by-product, to the detected signal. It was found that in the frequency range of interest below ca. 200 GHz (Josephson voltage $V < 400 \mu\text{V}$) this contribution is negligible, but it was increasing towards higher voltages across the junction, corresponding to the quasiparticle branch of the IV-curve.

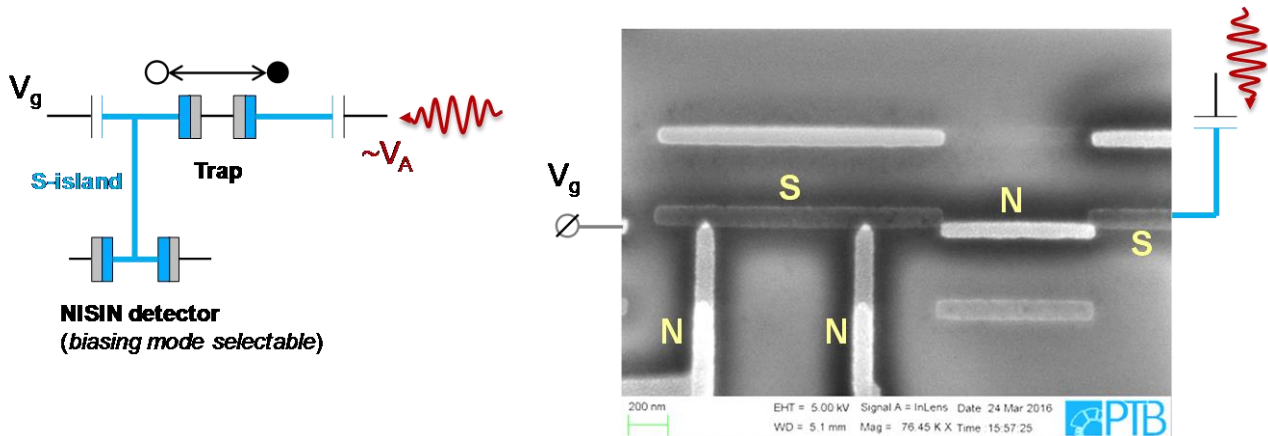


Figure 3.2.5.6. Equivalent circuit and SEM image of the joint SINIS+NISIN photon detector. Differently from the previously studied SINIS-trap plus SET-electrometer device, it includes a direct galvanic joint of the trapping S-island to the S-island of the NISIN SET transistor. For high intensities of the microwave signal V_A the trap plays a role of the “quasiparticle injector” for the NISIN detector. For low counting rates, the NISIN SET transistor is used to resolve single electron hopping events across the trap. In the SEM image, the dark replica is Al and the brighter replica is AuPd. “S”, blue = superconductor, “N”, grey = normal conducting.

Finally, PTB elaborated a design, fabricated the first family of samples and investigated at low temperatures a joint SINIS+NISIN detector circuit, shown in Figure 3.2.5.6, combining in a single device both operating principles and thus covering the full range of PAT counting rates from about 1 and up to 1000 photons per second. In measurements, the operation in the “NISIN-mode” has been achieved, while no discrete electron hopping has been observed yet, in the regime of electron trapping. This study will require further efforts, now outside of the scope of the project.

3.2.6 Superconducting transmon qubit -based source and SNS detector

The most challenging and risky target of the MICROPHOTON project was the integration of an on-demand single-photon source with a detector that can detect microwave photons with a good quantum efficiency. Aalto University has taken up the challenge of developing such an integrated source and detector device, which is sometimes referred to as an ‘on-chip quantum optics laboratory’, actually meaning a platform for performing microwave photonics and low level heat transport experiments. The transmon-qubit-based single-electron source (MkII) described in Section 3.2.1 was developed especially for that purpose in collaboration with Lancaster University. In addition to the SNS detector described in Section 3.1.3, Aalto has recently invented and studied another type of a detector, a dispersive thermometer, that also has great potential as a microwave photon detector.⁵ Experience obtained in that work has benefitted the design of a compatible SNS detector for the integrated source-detector device.

Experimental efforts towards the detection of qubit-sourced microwave photons with a mesoscopic square-law thermal detector based on an SNS element are in progress at Aalto. Although even the initial experimental results of this endeavour will be outside of the timeframe of the MICROPHOTON project, Aalto has completed the designs of compatible source and detector chips and started their fabrication. Figure 3.2.6.1 shows fabricated source and detector elements together with the designed layout of the source-detector experiment.

⁵ O.P. Saira et al., Phys. Rev. Appl. 6, 024005 (2016).

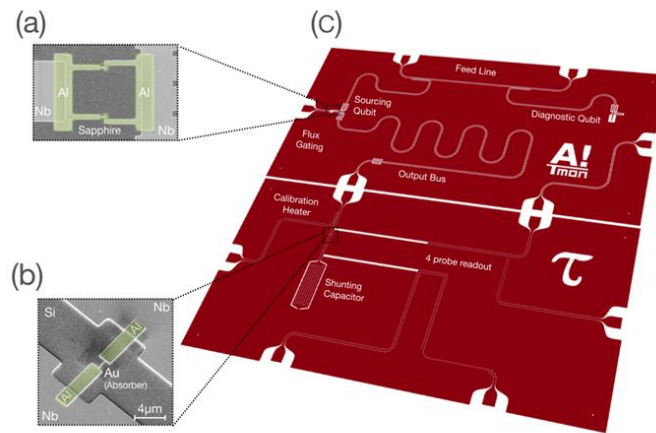


Figure 3.2.6.1. (a) SEM image of a fabricated photon sourcing junction. (b) SEM image of a gold absorber in an SNS detector. (c) Layout of the hybrid source-detector experiment. The top half houses a transmon qubit with microwave lines for state manipulation and readout, and a flux gating line to initiate rapid transfer of a single-photon excitation to a dedicated output resonator. In the bottom half, the incident microwave power is channelled to a simple SNS wire whose impedance has a dissipative component at microwave frequencies. This allows high-resolution single-shot threshold detection of the wire temperature with quasi-dc readout.

For the photon sourcing, the design includes a dedicated output resonator into which a single-photon excitation can be transferred from the transmon qubit with a few-ns flux pulse. This output resonator is designed to decay into a transmission line that is terminated by an SNS element. The source and detector chips can be fabricated independently, which results in the simplification of the fabrication process and allows independent testing of the respective parts. The SNS element will absorb the microwave excitation with high probability, as it is by design the dominating dissipative element for the output mode. The resulting temperature increase can be detected by a quasi-dc ($\sim 1 \mu\text{s}$ duration) current pulse, which realises as a sensitive threshold detection of the critical current of the wire, and hence of its temperature. The performance of the single-photon sourcing and detection scheme can be verified by studying the detector count rates as a function of the time delay between the photon release and temperature probe pulse, as well as the amplitude and duration of the flux pulse implementing the transfer of the excitation to the output resonator.

Additionally, with the expertise of the Low Temperature Laboratory and OtaNano research infrastructure at Aalto, we have assembled a measurement setup capable of measuring this integrated device at cryogenic temperatures with a combination of DC and attenuated high frequency wiring with low noise cryogenic amplification contained within a magnetically shielded controlled photonic environment.

3.2.7 Summary of microwave photon sources

In summary, two types of qubit-based on-demand sources of single microwave photons have been developed in this project. One of them is based on a transmon qubit and is rather similar to qubit-based single-photon sources developed earlier by other groups. The other one has a novel design and is unique in the sense that the frequency of generated photons can be tuned on a rather wide frequency range from 6.7 GHz to 9.1 GHz. Both devices are suitable for integrating with, e.g., an SNS-type thermal detector. Detection of microwave photons generated with an on-chip on-demand source would be a breakthrough in circuit quantum electrodynamics. Additionally, an on-chip microwave generator based on the Josephson generation phenomenon was developed and applied in the characterisation of SINIS trap detectors on the same chip.

3.3 Objective 3: Characterisation and minimisation of background microwave radiation in the cryogenic measurement systems of nanoelectronic devices. The goal is to decrease the background microwave radiation to a level which corresponds to the voltage noise of a SINIS-SET much below $1 \text{ pV/Hz}^{1/2}$ at frequencies above 10 GHz, simultaneously allowing bandwidth up to about 10 GHz for the control signals from room temperature to the cryo-electronic device.

An important motivation behind the development of microwave sensors that can detect effects caused by single photons was that such devices can be used to obtain information about the level and spectrum of microwave background radiation in cryogenic environments (objective 3 of the project). SINIS-type devices (Section 3.1.1) were developed and used for that purpose, as explained in Section 3.1.1. On the other hand, the background radiation can deteriorate the performance of many cryoelectronic devices, and the fourth objective of the project was to demonstrate improved performance when microwave background radiation is minimised.

VTT's technical activities in the project were mainly concentrated on work with background microwave radiation in cryogenic environments. The methods that were used to minimise the microwave radiation level in the experimental chamber are described in the Good practice guide for microwave radiation detection, shielding and filtering within cryogenic systems.

Objective 3 of the project was to develop methods to characterise and minimise the background microwave radiation in the cryogenic measurement systems. Cryogenic quantum devices are extremely sensitive to environmental fluctuations and, for example, quasiparticles excited by background microwave radiation are a serious problem for SINIS single-electron devices in many applications. The importance of minimising the level of background microwave radiation in the sample chamber by careful filtering and shielding has been demonstrated in earlier studies. In this project, VTT with input from Aalto designed and constructed a new sample chamber for studies of background microwave radiation (see Figure 3.3.1.1). It consists of six nested shields, which can be used to vary the level of shielding. However, in most experiments VTT used a more practical double-shielded sample holder shown in Figure 3.3.1.2. VTT with input from Aalto designed and implemented a so-called RF-SET (radio-frequency single-electron transistor) system in order to increase the photon counting bandwidth of the detector. For quantitative comparison of microwave background level with different shielding levels, it was planned to determine the rate of photon-induced tunnelling events in a double SINIS SET device. Several batches of double SINIS SET devices were fabricated, with different designs and fabrication parameters, but experiments at cryogenic temperatures indicated that the tunnel junctions of the devices were not ideal due to some fabrication problems, which could not be solved during the lifetime of the project. Tunnelling events caused by background microwave photons were overwhelmed by those caused by nonideal tunnel junctions, and quantitative studies of the microwave background level in different shielding conditions could not be performed.



Figure 3.3.1.1. The sample chamber designed for studies of the effects of microwave background radiation on the performance of cryogenic quantum devices. It consists of six nested shields, three of which are shown in the figure, which can be used to vary the level of shielding.

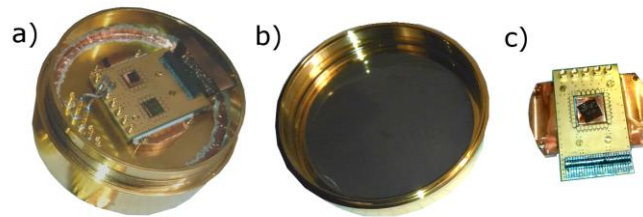


Figure 3.3.1.2. (a) Top view of the double-shielded sample chamber which was used in most experiments at VTT. A separate filtered entrance for wiring is underneath the copper plate. The seams are sealed with silver epoxy and copper tape and the plate is fixed with screws. (b) The inner shield of the sample chamber is covered with Eccosorb. (c) Sample holder.

SINIS SET devices can also be used to obtain spectral information about microwave radiation in cryogenic setups and devices. The threshold frequency of microwave radiation that can be observed by a SINIS single-electron trap detector can be adjusted by applied gate and bias voltages, which determine the threshold energy for photon-assisted tunnelling. Microwave photons from cryogenic background were coupled to the SINIS trap detector fabricated by PTB (see Figure 3.1.1.1) via two superconducting filters. The photon-assisted tunnelling rate of the SINIS trap was measured as a function of temperature with different values of applied control voltages to obtain spectral information of detected photons (see Figure 3.1.1.1d). Results were consistent with an attenuated Planck spectrum of a black-body emitter at 1.5 K before the filter elements (see Figure 3.3.1.3). The spectral response of the filters at frequencies between about 50 GHz and 200 GHz could be obtained from the measurement results together with circuit models of the filters [16].

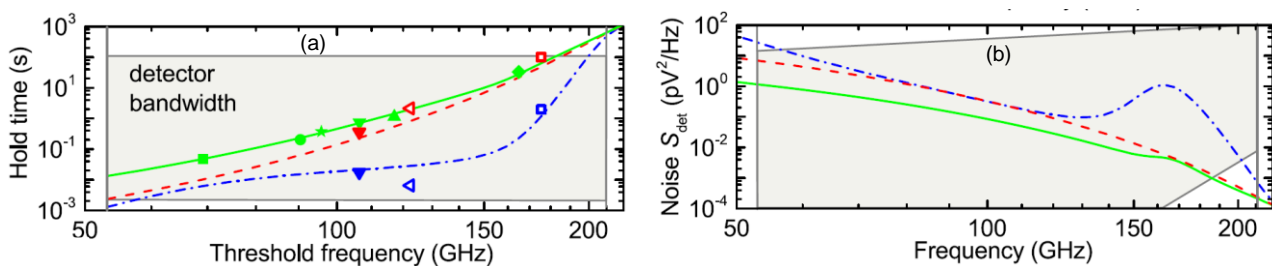


Figure 3.3.1.3. (a) The relation between the electron hold time and threshold frequency of the SINIS trap detector in different environmental conditions corresponding to different states of the filter (see Section 3.3.2): $B = 8$ mT and $T = 32$ mK (green solid line), $B = 0$ and $T > 100$ mK (red dashed line), and $B = 0$ and $T < 50$ mK (blue dashed-dotted line) [16]. The lines are based on fits of experimental data to theory assuming an attenuated Planck spectrum of a black-body emitter at 1.5 K before the filter elements. (b) Spectral density of microwave radiation reaching the detector in different experimental conditions using the same notation as in (a).

3.3.1 Summary of research on background microwave radiation in cryogenic environments

Cryogenic quantum devices are extremely sensitive to environmental fluctuations, for example quasiparticles excited by background microwave radiation are a serious problem for single-electron devices. According to the third objective of the project, methods were developed to characterise and minimise the background microwave radiation in cryogenic measurement systems. A measurement system with a variable level of microwave filtering and shielding was developed for systematic studies of the effects of microwave background radiation on cryoelectronic devices. The measurement system is available for measurements and has the potential to improve the performance of cryoelectronic quantum devices. However, quantitative measurements of the effects of different microwave background level on double SINIS-SET devices could not be performed due to sample fabrication problems. The project also demonstrated the usefulness of a SINIS trap detector as a tool for obtaining spectral information of microwave radiation and on-chip filters.

3.4 Objective 4: Demonstrations of the improved performance of cryoelectronic quantum nanodevices such as SINIS-SET-based components and other devices in which perfectness of superconductivity is important.

Objective 4 of the project is closely related to objective 3. In earlier work, partners of the project have been able to reduce the density of quasiparticles in superconducting aluminium of double SINIS SET devices to the record-low level of $0.033 \mu\text{m}^{-3}$ and to increase the stability time of electrons in a SINIS single-electron trap to above 10 hours by improved filtering and shielding. The idea in this project was to use the double SINIS SET device as a tool to demonstrate improved performance when filtering and shielding of the sample chamber are improved, but as was explained above, this plan was frustrated by technical problems in device fabrication.

However, some further evidence about improved performance of SINIS single-electron devices was obtained in experiments with the SINIS single-electron trap. The performance of the device was characterised by the hold time of electrons in the trap. VTT and PTB performed experiments with the same SINIS trap detector fabricated by PTB (see Figure 3.1.1.1). In VTT's new specially filtered and shielded measurement chamber (see Figure 3.3.1.2), the hold times of electrons in the trap were at least an order of magnitude longer (i.e. better) than in PTB's conventionally filtered and shielded cryostat. Moreover, the hold time could be varied by two orders of magnitude by the level of on-chip filtering by an external magnetic field.

PTB's SINIS trap detector devices that were used in the experiments have very small lateral dimensions on the scale of a few micrometres only, which is much smaller than, typically, millimetre-wavelengths of the microwave radiation. The SINIS trap detector of Figure 3.1.1.1 is supplied with two different on-chip filters connected in series: transmission line filters that are long (several millimetres) resistive (Ti) leads over the capacitive ground plane, and Josephson array filters that consist of a short ($\sim 10 \mu\text{m}$) array of small SQUIDs located in the direct vicinity of the SINIS trap (see Figure 3.1.1.1).

The attenuation of the Josephson array filter can be tuned by adjusting the critical current of the SQUID junctions by an applied magnetic field. As Figure 3.3.2.1a shows, the hold time of the electrons varies as a function of the magnetic field with a period of about 16 mT that corresponds to one magnetic flux quantum through the SQUID loop. When the magnetic field is increased from 0 mT to 8 mT, the hold time increases by two orders of magnitude, which means that the flux of background microwave photons that can reach the SINIS trap detector decreases by two orders of magnitude when the attenuation of the filter is tuned to its maximum. The measurement results can be understood by modelling the Josephson array filter as an RLC transmission line and assuming thermal spectrum for the microwave background radiation in the experimental chamber (with an effective temperature of 1.5 K instead of the sample temperature of about 30 mK).

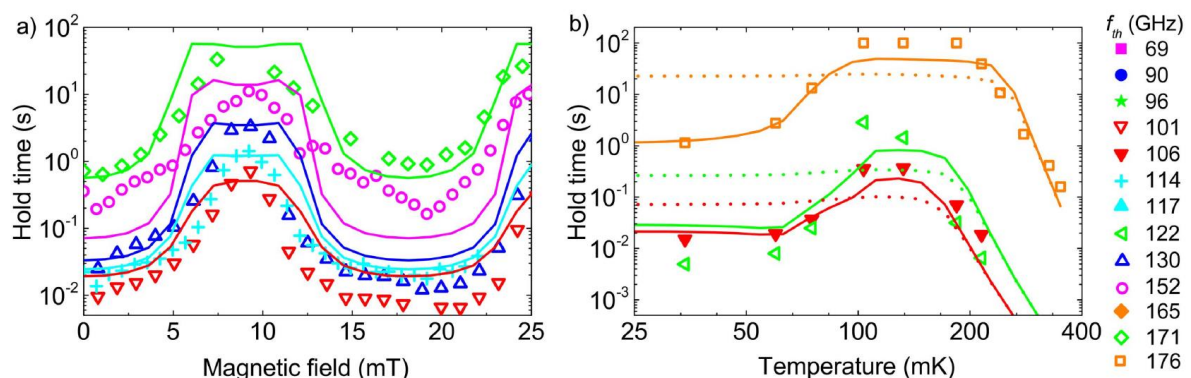


Figure 3.3.2.1. (a) Hold time of the SINIS trap as a function of magnetic field at different values of the SINIS trap's threshold energy for electron tunnelling (see Section 3.1.1) when $T = 32 \text{ mK}$. (b) Hold time of the SINIS trap as a function of temperature at different values of the SINIS trap's threshold energy for electron tunnelling when $B = 0$.

Somewhat surprisingly, the hold time of the trapped electrons starts decreasing rapidly with decreasing temperature when $T = 100 \text{ mK}$ is reached (see Figure 3.3.2.1b). At that temperature, titanium used in

transmission line filters becomes superconducting. When temperature decreases from 100 mK to 50 mK, the hold time of electrons in the trap decreases by about two orders of magnitude. Standard theories of microwave propagation in superconducting circuits would actually predict a small increase, instead of the large decrease, in the electron hold time when Ti becomes superconducting. However, VTT together with Aalto and PTB were able to explain the results of Figure 3.3.1.2b by modelling the Ti film as a disordered structure that consists of small weakly connected grains when titanium is superconducting.

3.4.1 Summary of research on improved performance of SINIS-SET based components

The aim of the fourth objective of the project was to use a double SINIS-SET device as a tool to demonstrate improved performance when increasing the filtering and shielding of the sample chamber. However, the work was frustrated by technical problems with device fabrication. The project did manage to obtain further evidence of the improved performance of SINIS single-electron devices in experiments with a SINIS single-electron trap detector. In the newly developed and specially filtered and shielded measurement chamber, the hold times of electrons in the trap were at least an order of magnitude longer than in a conventionally filtered and shielded cryostat. Moreover, a dramatic effect of filtering on the performance of SINIS single-electron devices was demonstrated in an experiment in which a SINIS single-electron trap was filtered by a (Superconducting QUantum Interference Device) SQUID array. The hold time could be increased by two orders of magnitude when on-chip filtering was improved by adjusting the external magnetic field to a value at which the SQUID array filter was blocked, thus preventing microwave photons penetrating via the on-chip leads.

3.5 Summary of research results

As a summary, the key results of research undertaken in the project include:

- Microwave photon detectors based on a SINIS-type single-electron trap were developed, and they were characterised using an on-chip microwave photon source based on Josephson junctions. As far as we know, this was the first time that individual microwave photons were generated by an on-chip source. The quantum efficiency of the SINIS-type photon detectors is very small, but the detector gives spectral information about the detected microwave photons.
- A single-shot electron detection scheme based on GaAs quantum dots was developed. The scheme has a potential use as a single microwave photon detector in the high frequency range (~ 200 GHz and above), but single-photon detection could not be demonstrated yet. The research undertaken is important for the development of quantum current standards and electron quantum optics, too.
- A thermal microwave photon detector based on a SNS (superconductor - normal metal - superconductor) structure was developed. In 'calorimetric' mode it achieved a resolution of approximately 200 microwave photons with a frequency of 8.4 GHz in a single shot corresponding to an energy sensitivity of approximately 1.1 zJ (zeptojoule), where $1 \text{ zJ} = 10^{-21} \text{ J}$. This is an order of magnitude improvement compared to earlier state of the art of thermal detectors, and it lays the foundation for ultrasensitive microwave bolometry and calorimetry and, ultimately, single-photon detection.
- The recently predicted phenomenon of period-doubling bifurcation (PDB) was observed experimentally for the first time. One benefit of the PDB-based microwave photon detectors is that they are expected to have better tuneability than the more conventional amplitude bifurcation amplifiers. Indeed, the fabricated PDB detectors have demonstrated expected switching behaviour in a wide range of tuning parameters. Sensitivity of PDB to microwave radiation was demonstrated, but not yet at the single-photon level.
- Superconducting transmon qubits in high-Q planar resonators were developed to be used as on-demand single-photon sources. In the second generation of the devices, measured coherence times $T_1 = 4.72 \mu\text{s}$ and $T_2 = 6.69 \mu\text{s}$ were similar to the state-of-the-art. After the end of the project, single-photon sourcing could be demonstrated in a similar experiment to Houck et al., Nature 449, 328 (2007). The first prototype of the transmon qubit source integrated with a variation of a SNS detector was also designed and partially fabricated, but the ultimate experiment to observe on-demand-generated single microwave photons with an on-chip single-photon detector could not be realised during the lifetime of the project.

- A novel microwave photon source based on a superconducting flux qubit coupled to a pair of transmission line waveguides was developed and its operation as an on-demand single-photon source was demonstrated. The unique property of the source is that the frequency of generated photons can be tuned on a wide frequency range between 6.7 GHz and 9.1 GHz. In this range, single-photon generation with an efficiency of at least 75 % was demonstrated. Single-photon generation was confirmed by measuring the second-order correlation function in a Hanbury-Brown-Twiss experiment. The result published in Nature Communications is scientifically very interesting and has large application potential e.g. in photonic quantum computers, highly sensitive detection, and metrology.
- More conventional cryogenic microwave sources based on the Josephson effect and on thermal effects have been developed as tools for testing the performance of microwave photon detectors. The Josephson sources were used successfully to test the performance of SINIS trap detectors in the frequency range from below 100 GHz up to about 200 GHz. However, perfect thermal microwave sources could not be fabricated due to technical problems, and microwave generation by that type of device could not be demonstrated.
- A measurement system with a variable level of microwave filtering and shielding was developed for systematic studies of the effects of microwave background radiation on cryoelectronic devices, and the usefulness of a SINIS trap detector as a tool for obtaining spectral information of microwave radiation and on-chip filters in cryogenic systems was demonstrated.
- Improved performance of a SINIS single-electron was demonstrated in an experiment in which a SINIS single-electron trap was filtered by a SQUID array. The hold time could be increased by two orders of magnitude when on-chip filtering was improved by adjusting the external magnetic field to a value at which the SQUID array filter was blocked, thus preventing microwave photons penetrating via the on-chip leads.
- Several new experimental facilities available for new research projects, were built at metrology institutes. They include measurement capabilities for second-order correlation functions of single microwave photon sources, a measurement system for studies of the effects of microwave background radiation on cryoelectronic devices, and an insert probe with a 180 GHz waveguide running from room temperature to the sample holder of a helium-3 cryostat for microwave photon-detection experiments.
- Fabrication facilities for nanodevices suitable for single-photon microwave detection and generation have been developed in several partner laboratories, and they are available for new research projects.

4 Actual and potential impact

The impact of this project is mostly in the scientific community, however, in the long-term, there will be financial and social impacts. The cryoelectronics market has already a significant volume of commercial applications, and this is expected to increase dramatically in future as the recent progress in cryogen-free refrigeration and on-chip coolers is making cryoelectronics more attractive for practical applications. Easy-to-use commercial methods for signal line filtering and radiation shielding of quantum nanodevices will benefit the manufacturers of cryogenic refrigerators and components.

Dissemination activities

Results of the project have been reported in 19 peer-reviewed publications and proceedings including highly ranked scientific journals such as Nature Communications and Physical Review Letters. A more general article about controlling single microwave photons was published in the Microwave Journal, which reaches 50,000 readers from all over the world. Project results have also been presented in 47 presentations or posters at scientific conferences and workshops.

In addition, the MICROPHOTON 2016 workshop covered quantum, microwave and cryogenic developments from the project and was attended by more than 60 participants from universities, research institutes, and the cryogenic and microwave industries.

The project website www.microphoton.eu and a newsletter were set-up as well as a stakeholder group. The stakeholder group was used to enhance dissemination of the outputs of the project and to provide opportunities for communication with target audiences.

On-line training on 'Shielding out high-energy photons inside a cryostat' was developed by the project and given to a group that actively works in this field at the University of Copenhagen. The training material is also available for stakeholders on the project website.

A good practice guide for microwave radiation detection, shielding and filtering within cryogenic systems has been produced and is available on the project website and via arXiv.

Impact on standards

Even though the work carried out in the project was of fundamental nature and not yet at the stage that needs standardisation, there was regular exchange of information about the project's progress with relevant technical committees particularly in the fields of electrical metrology and microwave science. The project was presented to the CIPM Consultative Committee for Electricity and Magnetism (CCEM) and to EURAMET Technical Committee for Electricity and Magnetism (TC-EM). More detailed results from the project have been given to the EURAMET TC-EM Subcommittee on DC and Quantum Metrology in 2015 and 2017. Project results were also presented for the International Union of Radio Science in the URSI Atlantic Meeting on Radio Science.

Early Impact

In this project, several nano- and cryoelectronic devices were developed which are important steps towards microwave photon detectors and on-demand sources. Substantial progress beyond the state of the art was achieved, and the work published in high-impact scientific journals has stimulated important further research in the field. Examples include:

- Demonstration of on-demand generation of single microwave photons with a tuneable frequency between 6.7 GHz and 9.1 GHz using a novel superconducting source based on a flux qubit coupled to a pair of transmission line waveguides. The result was published in Nature Communications has already been cited in at least 5 scientific articles.
- Improvement of the state-of-the-art of the sensitivity of thermal microwave photon detectors to the level of 1 zeptojoule (10^{-21} Joules), corresponding to approx. 200 photons at 8.4 GHz frequency, using an SNS detector. The result has already been cited in at least 7 published scientific articles.

The impact of the project for European quantum metrology is also significant:

- The project's new measurement capabilities for second-order correlation functions of single microwave photon sources will be an important tool in further research in microwave quantum optics.
- The project developed a measurement system which is available for studies of the effects of microwave background radiation on cryoelectronic devices.

- The project's research on the PBD amplifier lead to invention of a novel type of a Josephson traveling wave parametric amplifier.
- The project's development of a microwave photon detector based on a semiconductor quantum dot single-electron device has given important insight not only for microwave photon detection but also for applications of a similar device in so-called electron quantum optics.

Potential impact

Even though single-photon real-time detection with good fidelity was not achieved during the lifetime of the project, the achievement of this end goal is now closer. The microwave photon detectors and sources developed in this project have the potential to enable the realisation of a practical quantum computer based on solid-state qubits, which will be a revolutionary breakthrough.

5 Website address and contact details

The address of the project public website:

www.microphoton.eu

The contact details of the project coordinator:

Dr. Antti Manninen
VTT Technical Research Centre of Finland Ltd, Centre for Metrology MIKES
Tekniikantie 1, Espoo
P.O. Box 1000
FI-02044 VTT
Finland

Phone: + 358 40 514 8658
E-Mail: antti.manninen@vtt.fi

6 List of publications

- [1] M. Khabipov, B. Mackrodt, R. Dolata, T. Scheller, and A.B. Zorin, Investigation of nonlinear superconducting microwave resonators including Nb Josephson junctions and SQUID, J. Phys.: Conf. Ser. 507, 042016 (2014), doi:10.1088/1742-6596/507/4/042016
- [2] G.Ithier, G.Tancredi, and P.J.Meeson, Direct spectrum analysis using a threshold detector with application to a superconducting circuit, New J. Phys. 16, 055010 (2014), doi:10.1088/1367-2630/16/5/055010
- [3] J. Govenius, R. E. Lake, K. Y. Tan, V. Pietilä, J. K. Julin, I. J. Maasilta, P. Virtanen, and M. Möttönen, Microwave nanobolometer based on proximity Josephson junctions, Phys. Rev. B 90, 064505 (2014), doi:10.1103/PhysRevB.90.064505
- [4] A.J. Manninen, A. Kemppinen, E. Enrico, M. Kataoka, T. Lindström, A.B. Zorin, S.V. Lotkhov, M. Khabipov, M. Möttönen, R.E. Lake, J. Govenius, J.P. Pekola, Yu.A. Pashkin, P.J. Meeson, and O.V. Astafiev, Measurement and control of single-photon microwave radiation on chip, CPEM 2014 Conference Digest (2014), doi:10.1109/CPEM.2014.6898390
- [5] G.Ithier, G. Tancredi, and P.J. Meeson, Direct spectral analysis of environmental noise in SQUID and SQUBIT type circuits using a Josephson bifurcation amplifier, J. Phys.: Conf. Ser. 568, 052021 (2014), doi:10.1088/1742-6596/568/5/052021
- [6] G. Tancredi, G.Ithier, and P.J. Meeson, Spectroscopy of the modes of a non-linear superconducting microwave resonator via inter-mode coupling and bifurcation amplification, J. Phys.: Conf. Ser. 568, 052022 (2014), doi:10.1088/1742-6596/568/5/052022

- [7] J. Govenius, Y. Matsuzaki, I. G. Savenko, and M. Möttönen, Parity measurement of remote qubits using dispersive coupling and photodetection, *Phys. Rev. A* 92, 042305 (2015), doi:10.1103/PhysRevA.92.042305
- [8] Z.H. Peng, Yu-Xi Liu, J.T. Peltonen, T. Yamamoto, J.S. Tsai, and O. Astafiev, Correlated emission lasing in harmonic oscillators coupled via a single three-level artificial atom, *Phys. Rev. Lett.* 115, 223603 (2015), doi:10.1103/PhysRevLett.115.223603
- [9] B. Jalali-Jafari, S. Lotkhov, and A.B. Zorin, Detection of on-chip generated weak microwave radiation using superconducting normal-metal SET, *Appl. Sci.* 6, 35 (2016), doi:10.3390/app6020035
- [10] S. Lotkhov, B. Jalali-Jafari, and A.B. Zorin, Photon-activated electron hopping in a single-electron trap enhanced by Josephson radiation, *Appl. Phys. Lett.* 108, 172603 (2016), doi:10.1063/1.4948258
- [11] E. Enrico and F. Giazotto, Superconducting quantum interference single-electron transistor, *Phys. Rev. Applied* 5, 064020 (2016), doi:10.1103/PhysRevApplied.5.064020
- [12] J.S. Lehtinen, E. Mykkänen, A. Kemppinen, and A. Manninen, Methods for characterization and minimization of microwave background in cryogenic environment, *CPEM 2016 Conference Digest* (2016), doi:10.1109/CPEM.2016.7540789
- [13] J. Govenius, R.E. Lake, K.Y. Tan, and M. Möttönen, Detection of zeptojoule microwave pulses using electrothermal feedback in proximity-induced Josephson junctions, *Phys. Rev. Lett.* 117, 030802 (2016), doi:10.1103/PhysRevLett.117.030802
- [14] Z.H. Peng, S.E. de Graaf, J.S. Tsai, and O.V. Astafiev, Tunable on-demand single-photon source in the microwave range, *Nature Communications* 7, 12588 (2016), doi:10.1038/ncomms12588
- [15] A.B. Zorin, Josephson traveling-wave parametric amplifier with three-wave mixing, *Phys. Rev. Applied* 6, 034006 (2016), doi:10.1103/PhysRevApplied.6.034006
- [16] J.S. Lehtinen, E. Mykkänen, A. Kemppinen, D. Golubev, S.V. Lotkhov, and A.J. Manninen, Characterising superconducting filters using residual microwave background, *Supercond. Sci. Technol.* 30, 055006 (2017), doi:10.1088/1361-6668/aa63bc
- [17] R.E. Lake, J. Govenius, R. Kokkonen, K.Y. Tan, M. Partanen, P. Virtanen, and M. Möttönen, Microwave admittance of gold-palladium nanowires with proximity-induced superconductivity, *Adv. Electron. Mater.* 3, 1600227 (2017), doi:10.1002/aelm.201600227
- [18] R.E. George, J. Senior, O.-P. Saira, S.E. de Graaf, T. Lindstrom, J.P. Pekola, and Yu.A. Pashkin, Multiplexing superconducting qubit circuit for single microwave photon generation, *J. Low Temp. Phys.* 189, 60 (2017), doi: 10.1007/s10909-017-1787-x
- [19] T. Lindström, R. Lake, Yu.A. Pashkin, and A. Manninen, Controlling single microwave photons: a new frontier in microwave engineering, *Microwave Journal*, Vol. 60, Ed. 05 (2017).